Supporting Information

for

Controlling the Excited-State Relaxation for Tunable Single-Molecule Dual Fluorescence Both in the Solution and Film States

Gang Wang,† Nannan Ding,† Hongxing Hao, Qingwei Jiang, Qianqian Feng, Ke Liu, Chunxia Hua, Hongtao Bian,* Yu Fang and Fengyi Liu*

Key Laboratory of Applied Surface and Colloid Chemistry of Ministry of Education, Key Laboratory for Macromolecular Science of Shaanxi Province, School of Chemistry & Chemical Engineering, Shaanxi Normal University, Xi'an, Shaanxi 710062, P. R. China

E-mail: fengyiliu@snnu.edu.cn
htbian@snnu.edu.cn

† These authors contributed equally.

Table of Contents

Part I. Experimental methods

Reagents and materials

2-Aminothiophenol (TCI, >97.0%), 2-amino-4-methoxybenzoic acid (TCI, >98.0%), triphenyl phosphite (TCI, >97.0%), tetrabutylammonium bromide (TCI, >98.0%), 2-amino-5-methylbenzoic acid (TCI, >98.0%), 2-amino-5-cyanobenzoic acid (Ark, >97.0%), benzoyl chloride (innochem, >99.0%) were obtained commercially. All the solvents used for ultraviolet-visible (UV-vis) absorption, fluorescence spectroscopy and femtosecond transient absorption (TA) spectra measurements were freshly distilled before use. All the reagents were of analytical grade and directly used without purification or treatment unless specified otherwise.

Measurements

The ^{1}H NMR spectra of the synthesized compounds were recorded on a Bruker Avance 600 NMR spectrometer using tetramethylsilane (TMS, δ = 0 ppm) as an internal standard. The MS were obtained on a Bruker maxis UHR-TOF mass spectrometer in ESI positive mode. UV-vis absorption spectra were acquired on a JASCO 770V spectrometer. Steady-state fluorescence excitation and emission spectra were measured on a time-correlated single photon counting fluorescence spectrometer (Edinburgh Instruments FLS920) with Xenon lamp as the light source at ambient temperature except temperature-dependent emission measurements. Low temperatures were accomplished with the use of a nitrogen-flow Cryostat (Oxford OptistatDN), and the temperature was controlled at a precision level of 0.1 K by using the Oxford ITC503 temperature controller. The absolute fluorescence quantum yields were collected on the Hamamatsu C9920 Quantum Efficiency Measurement. Crystallographic data for the compounds were collected on a BRUKER APEX-II CCD diffractometer. Ga Kα (λ = 1.34139 Å) for M-OMe and M-Me and Mo Kα (λ = 0.71073 Å) for M-CN was used as the radiation source to collect X-ray reflections from the single crystal mounted on the X-ray machine. The crystallographic data (including the structure factor files) for M-OMe, M-Me and M-CN in present work have been deposited in the Cambridge Crystallographic Data Centre as a supplementary publication with CCDC Nos. 2101306-2101308. The surface morphologies of the fluorescence films were examined on a field emission scanning electron microscope (SU8020, Hitachi) at an acceleration voltage of 3 kV, and all samples were coated with gold.

The samples used for femtosecond transient absorption (TA) spectra measurements were prepared in a quartz cell with side length 2 mm. The TA spectra were obtained on the transient absorption pump-probe spectrometer (Keramiku 2B, LT-10233). The pulsed light at 800 nm (1 kHz repetition rate) was produced by a regenerative amplified Ti-sapphire laser system from HARPIA. The 800 nm output pulse was split into two parts. The transmitted part was applied to pump an Optical Parametric Amplifier (OPA). The reflected 800 nm beam was split again into two parts. One part of the 800 nm pulse was attenuated with a neutral density filter and then focused onto a 2 mm-thick sapphire window to produce a white light continuum (WLC), which affords a usable probe spectral range between 355 nm and 680 nm. The TA spectra were collected at magic angle (54.7°) of pump and probe beam polarization to eliminate anisotropy.

Fabrication of the fluorescence film

The compound was dissolved into dichloromethane. Then, a certain volume of *n*-hexane, in which the compound has limited solubility, was rapidly added to the dichloromethane solution. The final concentration of the compound was 1.0 mmol/L and the volume ratio of dichloromethane to *n*-hexane was 2:3. After standing for 30 minutes, a defined amount (60 μL) of the resulting mixture was drop-casted on a clean glass substrate, and dried in air at room temperature to yield the fluorescence films used for spectral measurements. The samples for scanning electron microscopy (SEM) measurements were prepared by drop-casting the as-prepared mixed solution onto a clean silicon plate surface. The well-defined self-assembled structure of the compound on the film surface is formed. The thickness of the fluorescence film of M-CN, M-Me and M-OMe is around 10 μm, 30 μm and 6 μm, respectively (Figs. S20, S21 and S22).

Part II. Computational details

All the (TD-)DFT calculations with the PBE0 functional[S1] were performed using the Gaussian 09 program package.[S2] A 6-31G(d,p) basis set was used,[S3] combined with the polarizable continuum model (PCM)[S4] to take the solvent effects (dichloromethane, ε = 8.93) into account. To validate the ground-state optimized geometries as minimum points, vibrational frequency calculations were carried out. To explore the excited-state intramolecular proton transfer (ESIPT) and other excited-state deactivation processes, S_0 and S_1 potential energy surfaces (PESs) were constructed via a series of constrained geometry optimizations which set one geometry parameter (the N1-H6 distance, the N1-C2-C3-C4 (α) and C4-N5-C7-C8 (β) dihedral angle) as a fixed value and relaxed all other geometry parameters. Moreover, to deeply understand the anomalous fluorescence properties of M-OMe, S_2 PES was calculated using the same method. For the excited-state geometry optimizations, the linear-response (LR) solvation formalism[S5] was employed. Meanwhile, PCM with a state-specific (SS)[S6] solvation correction was adopted to calculate the absorption wavelength. To verify the computational results of the present systems calculated by the PBE0 functional, the calculation of the absorption wavelengths based on the correspondingly optimized S_0 geometries and construction of S_0 and S_1 PESs of three studied dyes have been carried out using PBE0-D3[S7]. The same basis set was employed. The results are displayed in Tables S2 and Figs. S23, S24 and S25. It can be seen that the calculated absorption maxima as well as S_0 and S_1 energy profiles of three fluorophores using PBE0 are almost the same as those obtained with PBE0-D3. Accordingly, the calculation results computed by the PBE0 functional are reasonable. The electron-hole distributions corresponding to the $S_0 \rightarrow S_1$ and $S_0 \rightarrow S_2$ transitions at Frank-Condon points were analyzed using the Multiwfn program (version 3.6).[S8]

To simulate the ground- and excited-state PESs of the studied fluorophores in the film state, the combined quantum mechanics and molecular mechanics (QM/MM) method with a two-layer ONIOM approach was used. For ONIOM calculations, the initial structures were the clusters containing 54 molecules that were extracted from the crystal of three compounds (displayed in the Supporting Information), of which one molecule in the center of the surface was set as the model part and treated by high-level QM calculation at (TD-)PBE0/6-31G(d,p) level, and the others were computed by low-level UFF force field[S9] with QEQ[S10] charges. Furthermore, only the molecule in the high-level layer (QM region) can move during the geometric optimizations, while the fluorophores in low-level layer are frozen. The setups of computational model of three compounds are shown in Figs. S26, S27 and S28.

(S1) C. Adamo and V. Barone, Toward Reliable Density Functional Methods without Adjustable Parameters: The PBE0 Model, *J. Chem. Phys.*, 1999, **110**, 6158-6170.

(S2) M. J. Frisch, G. W. Trucks, H. B. Schlegel, G. E. Scuseria, M. A. Robb, J. R. Cheeseman, G. Scalmani, V. Barone, B. Mennucci, G. A. Petersson, et al. *Gaussian 09*, revision D. 01. Gaussian, Inc.: Wallingford, CT, 2009.

(S3) M. M. Francl, W. J. Pietro, W. J. Hehre, J. S. Binkley, M. S. Gordon, D. J. DeFrees and J. A. Pople, Self-consistent Molecular Orbital Methods. XXIII. A Polarization-Type Basis Set for Second-Row Elements, *J. Chem. Phys.*, 1982, **77**, 3654-3665.

(S4) J. Tomasi, B. Mennucci and R. Cammi, Quantum Mechanical Continuum Solvation Models. *Chem. Rev.*, 2005, **105**, 2999-3093.

(S5) G. Scalmani, M. J. Frisch, B. Mennucci, J. Tomasi, R. Cammi and V. Barone, Geometries and Properties of Excited States in the Gas Phase and in Solution: Theory and Application of A Time-Dependent Density Functional Theory Polarizable Continuum Model, *J. Chem. Phys.*, 2006, **124**, 094107.

(S6) R. Improta, V. Barone, G. Scalmani and M. J. Frisch, A State-Specific Polarizable Continuum Model Time Dependent Density Functional Fheory Method for Excited State Calculations in Solution, *J. Chem. Phys.*, 2006, **125**, 054103.

(S7) S. Grimme, J. Antony, S. Ehrlich and H. Krieg, A Consistent and Accurate *ab initio* Parametrization of Density Functional Dispersion Correction (DFT-D) for the 94 Elements H-Pu, *J. Chem. Phys.*, 2010, **132**, 154104.

(S8) T. Lu and F. W. Chen, Multiwfn: A Multifunctional Wavefunction Analyzer, *J. Comput. Chem.*, 2012, **33**, 580-592.

(S9) A. K. Rappé, C. J. Casewit, K. S. Colwell, W. A. Goddard III, W. M. Skiff, UFF, A Full Periodic Table Force Field for Molecular Mechanics and Molecular Dynamics Simulations, *J. Am. Chem. Soc.*, 1992, **114**, 10024-10035.

(S10) A. K. Rappé and W. A. Goddard III, Charge Equilibration for Molecular Dynamics Simulations, *J. Phys. Chem.*, 1991, **95**, 3358-3363.

Part III. Synthesis and characterization

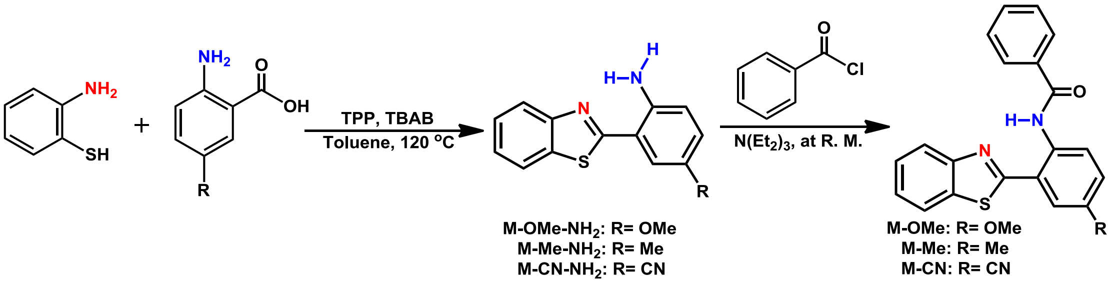

The synthesis routes of M-OMe, M-Me and M-CN.

M-OMe-NH$_2$: 2-aminothiophenol (0.25 g, 2.0 mmol), 2-amino-4-methoxybenzoic acid (0.34 g, 2.0 mmol), triphenyl phosphite (TPP, 0.62 g, 2.0 mmol) and tetrabutylammonium bromide (TBAB, 0.77 g, 2.4 mmol) in toluene (20 mL) under nitrogen atmosphere was stirred at 120 °C for 20 h in a 50 mL round bottomed flask. After the reaction was finished (monitored by TLC), the reaction mixture was cooled to room temperature, and then filtrated. The filtrate was evaporated under reduced pressure. The residue was purified by flash column chromatography on silica gel with CH_2Cl_2/*n*-hexane (v/v, 1:2) followed by recrystallization from $CHCl_3$ and *n*-hexane to yield M-OMe-NH$_2$ as a white needle-like solid. ^{1}H NMR (CD_2Cl_2/Me_4Si, 600 MHz, Fig. S29), δ (ppm): 7.82 (d, *J*=8.4, 1H), 7.79 (d, *J*=7.8, 1H), 7.54 (d, *J*=9.0, 1H), 7.36 (t, *J*=7.8, 1H), 7.25 (t, *J*=8.4, 1H), 6.44 (s, 2H), 6.26 (d, *J*=9.0, 1H), 6.19 (s, 1H), 3.73 (s, 3H); MS (m/z), Calcd. for [(M + H)$^+$]: 257.0743, found: 257.0739.

M-Me-NH$_2$: The compound was synthesized according to the procedure for the preparation of M-OMe-NH$_2$, while 2-amino-4-methoxybenzoic acid was replaced by 2-amino-5-methylbenzoic acid as the starting material. The desired product, M-Me-NH$_2$, was obtained as a yellow powder. ^{1}H NMR ($CDCl_3$/Me_4Si, 600 MHz, Fig. S30), δ (ppm): 7.97 (d, *J*=7.8, 1H), 7.87 (d, *J*=7.8, 1H), 7.50 (s, 1H), 7.45 (m, 1H), 7.35 (m, 1H), 7.06 (d, *J*=8.4, 1H), 6.73 (d, *J*=8.4, 1H), 2.31 (s, 3H); MS (m/z), Calcd. for [(M + H)$^+$]: 241.0794, found: 241.0794.

M-CN-NH$_2$: The compound was synthesized according to the procedure for the preparation of M-OMe-NH$_2$, while 2-amino-4-methoxybenzoic acid was replaced by 2-amino-5-cyanobenzoic acid as the starting material. The desired product, M-CN-NH$_2$, was obtained as a light yellow powder. ^{1}H NMR ($CDCl_3$/Me_4Si, 600 MHz, Fig. S31), δ (ppm): 8.01 (m, 2H), 7.93 (d, *J*=7.2, 1H), 7.50 (m, 1H), 7.42 (m, 2H), 6.80 (d, *J*=9.0, 1H); MS (m/z), Calcd. for [(M + H)$^+$]: 252.0590, found: 252.0588.

M-OMe: Benzoyl chloride (0.20 mL, 1.7 mmol) was quickly injected into a stirred solution of triethylamine (0.26 mL, 1.9 mmol) and M-OMe-NH$_2$ (43.30 mg, 0.17 mmol) in chloroform (50 mL) under nitrogen atmosphere at room temperature. The resulting mixture was continuously stirred for 6 h. Then, the solvent was removed by rotary evaporation under reduced pressure, and the mixture was purified by flash column chromatography on silica gel with CH_2Cl_2/*n*-hexane (v/v, 1:2) followed by recrystallization from $CHCl_3$ and *n*-hexane to afford M-OMe as a white needle-like crystal. ^{1}H NMR (CD_2Cl_2/Me_4Si, 600 MHz, Fig. S32), δ (ppm): 13.42 (s, 1H), 8.63 (s, 1H), 8.16 (d, *J*=7.2, 2H), 7.91 (d, *J*=8.4, 1H), 7.85 (d, *J*=8.4, 1H), 7.76 (d, *J*=8.4, 1H), 7.55 (m, 3H), 7.46 (t, *J*=7.2, 1H), 7.35 (t, *J*=7.8, 1H), 6.69 (d, *J*=9.0, 1H), 3.86 (s, 3H); MS (m/z), Calcd. for $[(M + H)^+]$: 361.1005, found: 361.1001. Crystallographic refinement data and crystal structure are shown in Table S6 and Fig. S35.

M-Me: The compound was synthesized according to the procedure for the preparation of M-OMe, while M-OMe-NH_2 was replaced by M-Me-NH_2 as the starting material. The desired product, M-Me, was obtained as a white needle-like solid. ^{1}H NMR (CD_2Cl_2/Me_4Si, 600 MHz, Fig. S33), δ (ppm): 13.15 (s, 1H), 8.83 (d, *J*=8.4, 1H), 8.13 (d, *J*=6.6, 2H), 7.95 (d, *J*=8.4, 1H), 7.89 (d, *J*=7.8, 1H), 7.68 (s, 1H), 7.54 (m, 4H), 7.38 (t, *J*=7.8, 1H), 7.30 (d, *J*=8.4, 1H), 2.35 (s, 3H); MS (m/z), Calcd. for $[(M + H)^+]$: 345.1056, found: 345.1051. Crystallographic refinement data and crystal structure are shown in Table S7 and Fig. S36.

M-CN: The compound was synthesized according to the procedure for the preparation of M-OMe, while M-OMe-NH_2 was replaced by M-CN-NH_2 as the starting material. The desired product, M-CN, was obtained as a white needle-like solid. ^{1}H NMR ($CDCl_3$/Me_4Si, 600 MHz, Fig. S34), δ (ppm): 13.64 (s, 1H), 9.22 (d, *J*=8.4, 1H), 8.22 (m, 3H), 8.04 (d, *J*=8.4, 1H), 7.99 (d, *J*=7.8, 1H), 7.79 (m, 1H), 7.63 (m, 4H), 7.52 (m, 1H); MS (m/z), Calcd. for $[(M + H)^+]$: 356.0852, found: 356.0840. Crystallographic refinement data and crystal structure are shown in Table S8 and Fig. S37.

Part IV. Supplementary data

Table S1. Photophysical properties of M-CN, M-Me and M-OMe in dichloromethane solution and film states at ambient temperature. The absolute fluorescence quantum yields and lifetimes were obtained upon the excitation at 345 nm.

	λ_{abs}/nm (solution) (ε [$M^{-1}cm^{-1}$])	**λ_{em}/nm**		**Φ_f**		τ (ns)	
		Sol.	**Film**	**Sol.**	**Film**	**Sol.**	**Film**
M-CN	284 (3.6×10^{-4})	399 (N^*)	422 (N^*)	7.2%	34.6%	— (N^*)	3.7 (N^*)
	343 (1.3×10^{-4})	550 (T^*)	528 (T^*)			~0.7 (T^*)	3.7 (T^*)
M-Me	279 (2.5×10^{-4})	411 (N^*)	436 (N^*)	2.1%	27.0%	— (N^*)	4.6 (N^*)
	351 (1.3×10^{-4})	570 (T^*)	568 (T^*)			~0.2 (T^*)	4.5 (T^*)
M-OMe	280 (3.2×10^{-4})	400 (N^*)	416 (N^*)	1.5%	49.9%	~0.1 (N^*)	3.4 (N^*)
	345 (2.7×10^{-4})	530 (T^*)	528 (T^*)			~0.2 (T^*)	4.1 (T^*)

Note: Sol. represents for the solution state, Φ_f the fluorescence quantum yield determined through using integrating sphere method, τ the fluorescence lifetime measured at 530 nm corresponding to the T^* emission in the dichloromethane solution and at 416 nm corresponding to the N^* emission in the film state upon the excitation at 340 nm. Time-resolved emission decay curves of three fluorophores are shown in Figs. S6, S7, S9 and S10. The fluorescence from the N^* emission of M-CN and M-Me is too weak so that their decays cannot be detected.

Table S2. Computed excitation energy, absorption wavelengths and oscillator strength of M-CN, M-Me and M-OMe in the N form involved in their corresponding $S_0 \rightarrow S_n$ (n = 1, 2, 3, 4, 5) transitions at the FC point, calculated at TD-PBE0/6-31G(d,p) level in dichloromethane calculated by different kind of functionals.

Absorption		**Functional**	**M-CN**	**M-Me**	**M-OMe**
$S_0 \rightarrow S_1$	Excitation energy	**TD-PBE0**	337 nm (3.68 eV)	349 nm (3.56 eV)	373 nm (3.32 eV)
	Oscillator strength		0.452	0.418	0.282
	Excitation energy	**TD-PBE0-D3**	338 nm (3.67 eV)	350 nm (3.55 eV)	374 nm (3.31 eV)
	Oscillator strength		0.439	0.408	0.276
$S_0 \rightarrow S_2$	Excitation energy	**TD-PBE0**	301 nm (4.12 eV)	300 nm (4.14 eV)	305 nm (4.07 eV)
	Oscillator strength		0.051	0.173	0.197
	Excitation energy	**TD-PBE0-D3**	300 nm (4.13 eV)	300 nm (4.14 eV)	305 nm (4.07 eV)
	Oscillator strength		0.054	0.173	0.188
$S_0 \rightarrow S_3$	Excitation energy	**TD-PBE0**	297 nm (4.18 eV)	287 nm (4.31 eV)	292 nm (4.24 eV)
	Oscillator strength		0.004	0.006	0.266
	Excitation energy	**TD-PBE0-D3**	297 nm (4.18 eV)	287 nm (4.31 eV)	292 nm (4.24 eV)
	Oscillator strength		0.002	0.004	0.281
$S_0 \rightarrow S_4$	Excitation energy	**TD-PBE0**	289 nm (4.28 eV)	283 nm (4.39 eV)	284 nm (4.36 eV)
	Oscillator strength		0.076	0.058	0.554
	Excitation energy	**TD-PBE0-D3**	289 nm (4.28 eV)	283 nm (4.38 eV)	285 nm (4.36 eV)
	Oscillator strength		0.062	0.051	0.553
$S_0 \rightarrow S_5$	Excitation energy	**TD-PBE0**	280 nm (4.43 eV)	277 nm (4.47 eV)	281 nm (4.42 eV)
	Oscillator strength		1.025	0.672	0.004
	Excitation energy	**TD-PBE0-D3**	280 nm (4.43 eV)	278 nm (4.47 eV)	281 nm (4.42 eV)
	Oscillator strength		1.056	0.690	0.001

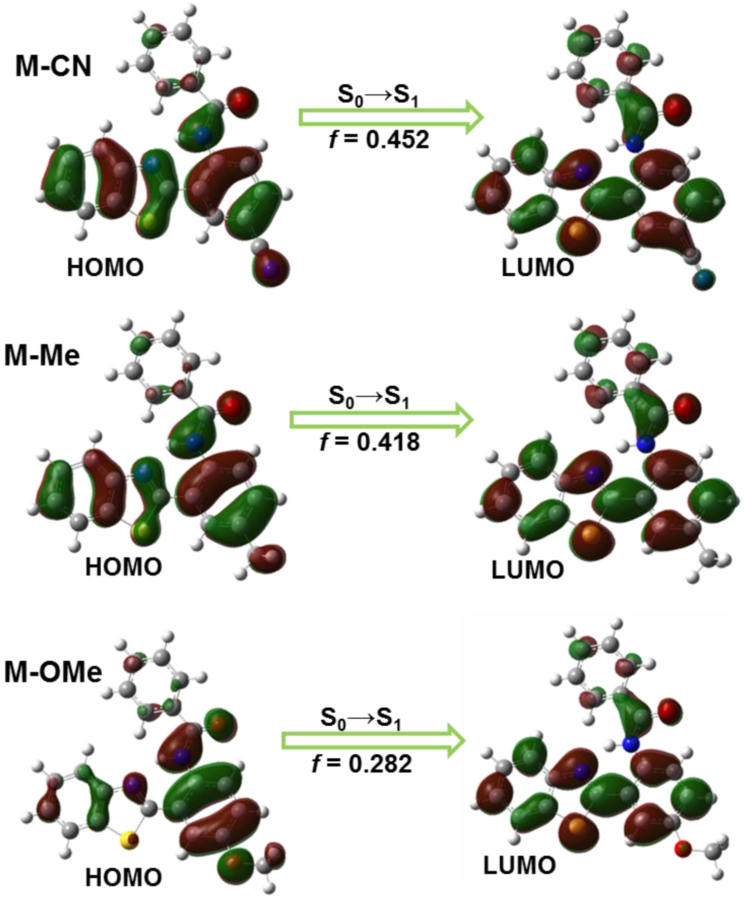

Fig. S1 Computed key orbitals (isovalue = 0.02), oscillator strength (*f*) of M-CN, M-Me and M-OMe in the N form involved in their corresponding $S_0 \rightarrow S_1$ transitions at the FC point, calculated at TD-PBE0/6-31G(d,p) level in dichloromethane.

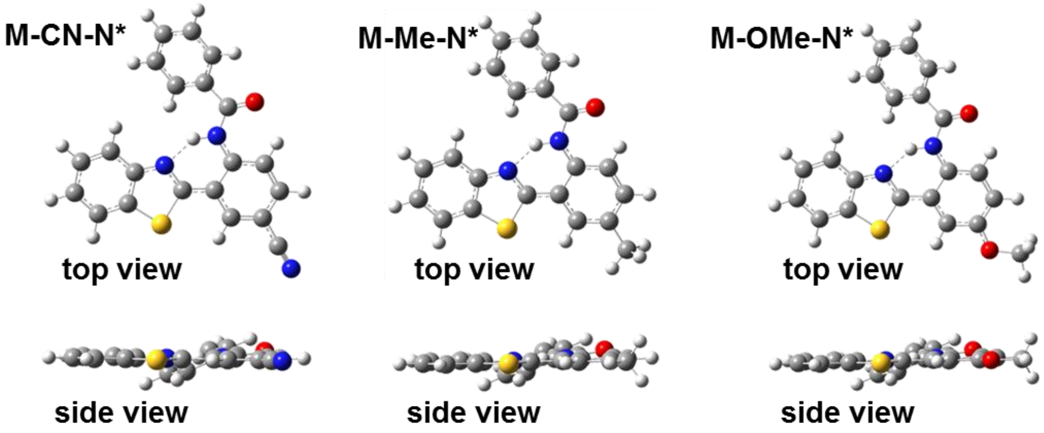

Fig. S2 Optimized S_1 geometrical structures of the synthesized ESIPT fluorophores with the N configuration at TD-PBE0/6-31G(d,p) level in dichloromethane.

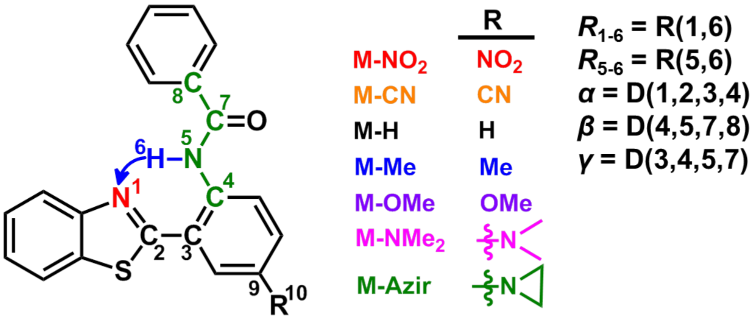

Table S3. Key geometry parameters (bond distances in angstroms and dihedral angles in degree) for the S_1 minima of the synthesized ESIPT fluorophores in dichloromethane.

Structure	Functional	α/ °	β/ °	γ/ °	$R_{1\text{-}6}$/Å	$R_{5\text{-}6}$/Å
M-CN-N	TD-PBE0	0.1	175.6	176.9	1.739	1.039
M-Me-N	TD-PBE0	0.0	174.8	176.8	1.720	1.043
M-OMe-N	TD-PBE0	-0.4	174.9	177.1	1.700	1.047
M-CN-T	TD-PBE0	-10.9	167.1	164.1	1.028	1.885
M-Me-T	TD-PBE0	-9.2	171.4	165.8	1.034	1.832
M-OMe-T	TD-PBE0	-5.8	172.7	168.8	1.041	1.780

Table S4. The energy difference between the normal form and its corresponding phototautomer of the synthesized ESIPT molecules at the S_1 minimum optimized at TD-PBE0/6-31G(d,p) level in dichloromethane solution and at the ONIOM(TD-PBE0:UFF) level in the film state, the energy difference is given in kcal/mol.

	M-CN		**M-Me**		**M-OMe**	
Phase	solution	Film	solution	Film	solution	Film
Δ*E*	0.4	-1.2	1.3	2.2	2.1	3.9

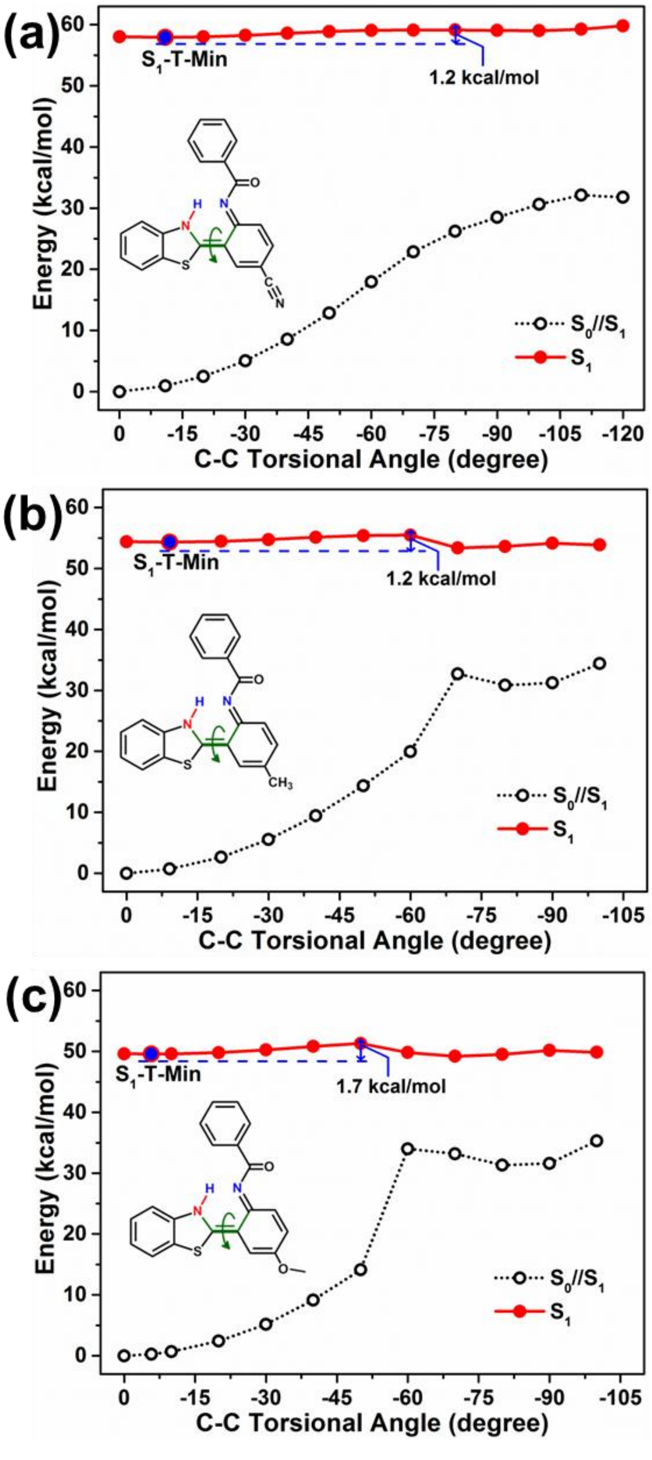

Fig. S3 Calculated S_0 and S_1 energy profiles of M-CN (a), M-Me (b) and M-OMe (c) in the phototautomeric form along with the C2-C3 torsional coordinates, optimized at TD-PBE0/6-31G(d,p) level in dichloromethane (S_1: the potential energy surface of the S_1 state; S_0//S_1: vertically projected S_0 energy on top of optimized S_1 geometries). The torsional angles are given in degrees.

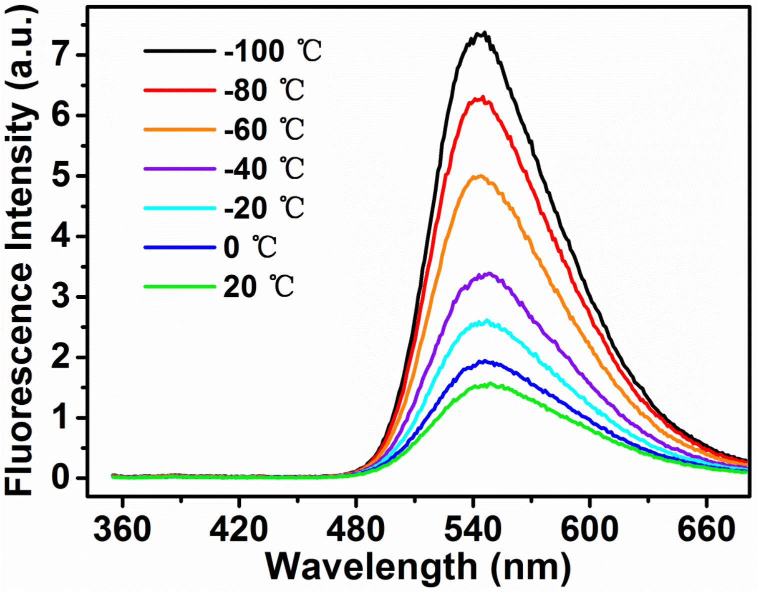

Fig. S4 Temperature-dependent fluorescence emission spectra of M-CN in dichloromethane recorded at a concentration of 1.0×10^{-5} mol/L upon the excitation at 345 nm.

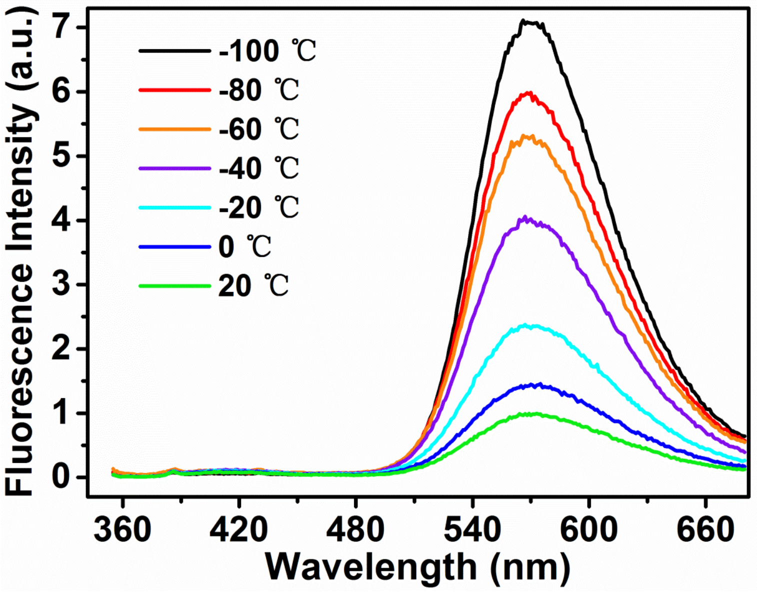

Fig. S5 Temperature-dependent fluorescence emission spectra of M-Me in dichloromethane recorded at a concentration of 1.0×10^{-5} mol/L upon the excitation at 345 nm.

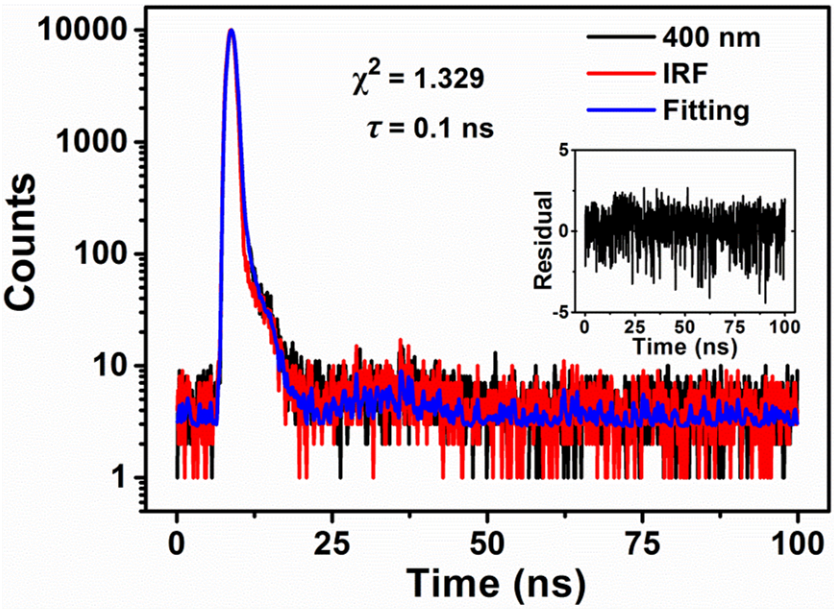

Fig. S6 Time-resolved emission decay curve monitored at 400 nm of M-OMe in dichloromethane at a concentration of 1.0×10^{-5} mol/L using pico-second pulsed diode laser (EPLED-340) as an excitation source. The insets are the corresponding residual-distributions. Note: Chi-square (χ^2) is a parameter to quantify the fitting quality.

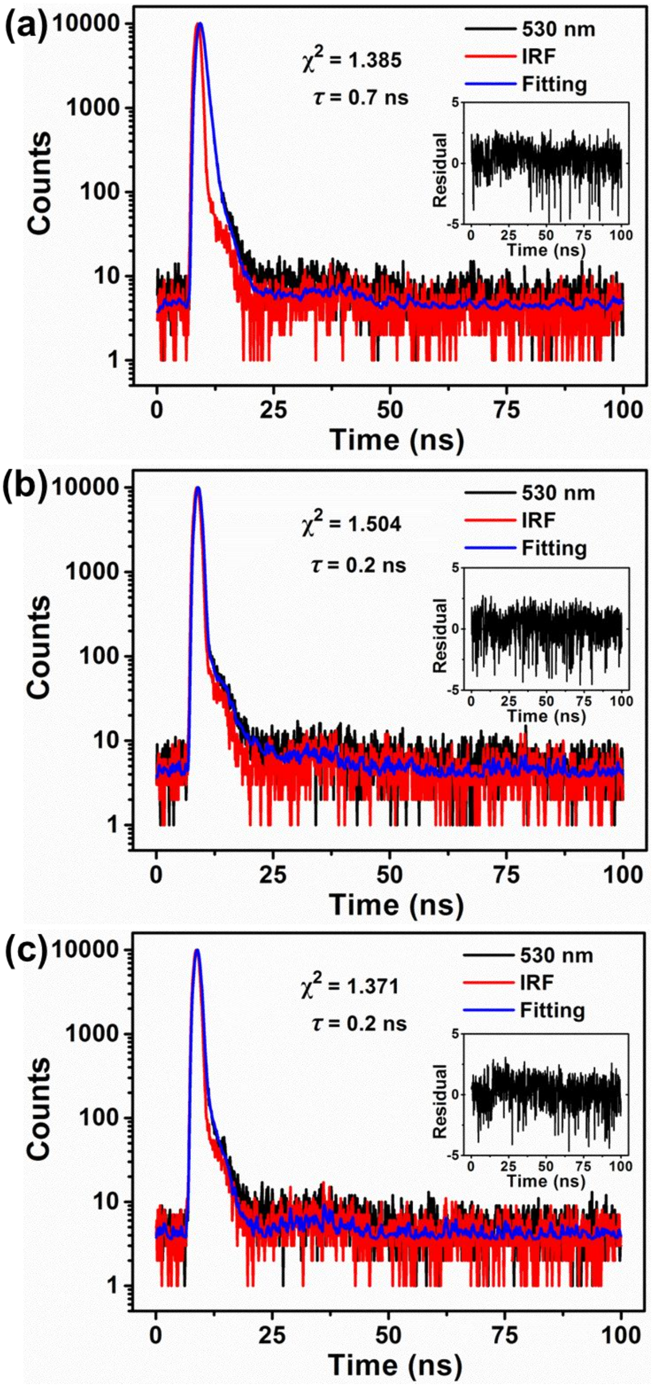

Fig. S7 Time-resolved emission decay curves monitored at 530 nm of M-CN (a), M-Me (b) and M-OMe (c) in dichloromethane at a concentration of 1.0×10^{-5} mol/L using pico-second pulsed diode laser (EPLED-340) as an excitation source. The insets are the corresponding residual-distributions. Note: Chi-square (χ^2) is a parameter to quantify the fitting quality.

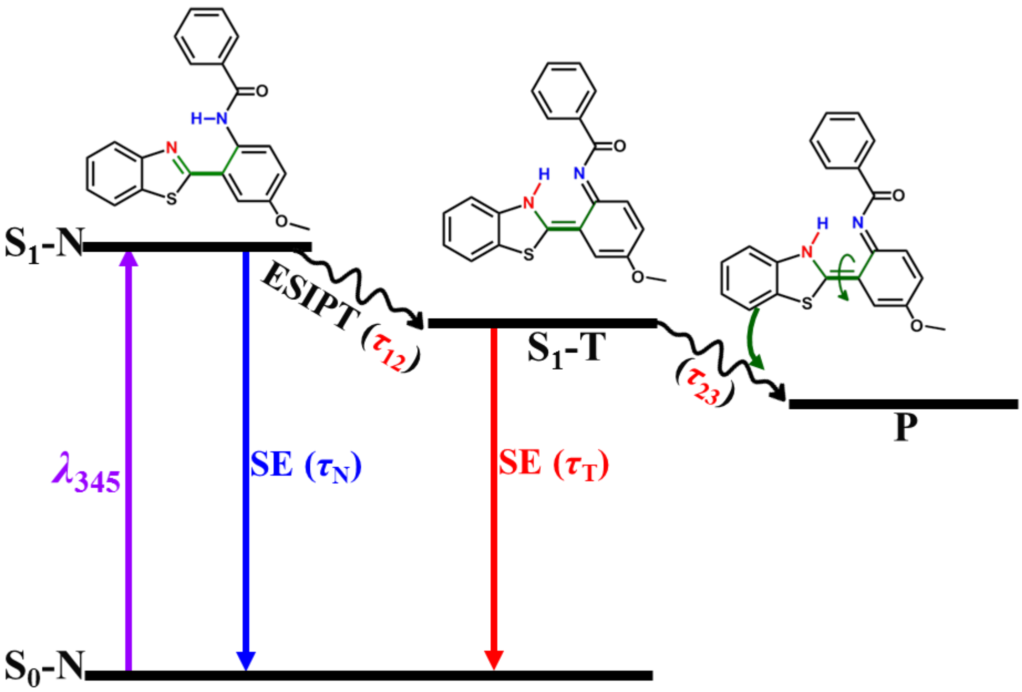

Scheme S1. Proposed relaxation pathways of M-OMe in dichloromethane upon the excitation at 345 nm, where S_0 and S_1-N stand for the components of M-OMe with the N configuration in the S_0 and S_1 states, S_1-T is representative of the ESIPT product of M-OMe in the S_1 state, and P is the photochemical product of S_1-T.

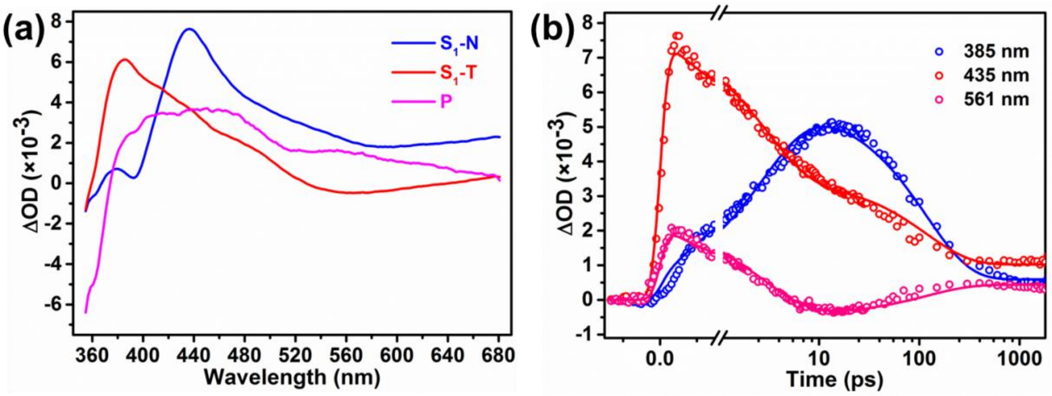

Fig. S8 Evolution-associated difference spectra for M-OMe in dichloromethane upon the excitation at 345 nm (a); Kinetics traces at selected wavelengths for M-OMe in dichloromethane with the excitation at 345 nm (b).

Table S5. Time constants extracted from global analysis of the TA data of M-OMe in dichloromethane upon the excitation at 345 nm.

λ_{abs}/nm	τ_{12}	τ_N	τ_T	τ_{23}
345	3.2 ps	27.0 ps	172.9 ps	373.3 ps

To shed light on the ESIPT dynamics of M-OMe, the global analysis of the TA data in dichloromethane was performed. Upon the excitation at 345 nm, two exponentially decaying components and one nondecaying component were essential for fitting the data. When 280 nm was used as the excitation wavelength, three exponentially decaying components and one nondecaying component were required to describe the data. The corresponding sequential model for global fitting was proposed as shown in Scheme S1. The results are exhibited as evolution-associated difference spectra (EADS) shown in Fig. S8a. The selected kinetics traces at different wavelengths of M-OMe in dichloromethane match well with the fitting curves at different wavelengths, as shown in Fig. S8b. All the corresponding time constants in dichloromethane are listed in Table S5. Upon the excitation at 345 nm, the lifetime constant of 3.2 ps (τ_{12}) is attributed to the fast ESIPT process. 27.0 ps (τ_N) and 172.9 ps (τ_T) can be assigned to the N^* and T^* decay, respectively. 373.3 ps can be considered as another possibly non-radiative process including the torsional motion around C2-C3 bond of the ESIPT product. Comparative analysis on the lifetime constants reveals that ESIPT occurs in 3.2 ps, and fluorescence emission as well as the non-radiative C2-C3 bond torsion of M-OMe is extremely fast. Therefore, the emission properties of the compound in the solution state should be kinetically controlled.

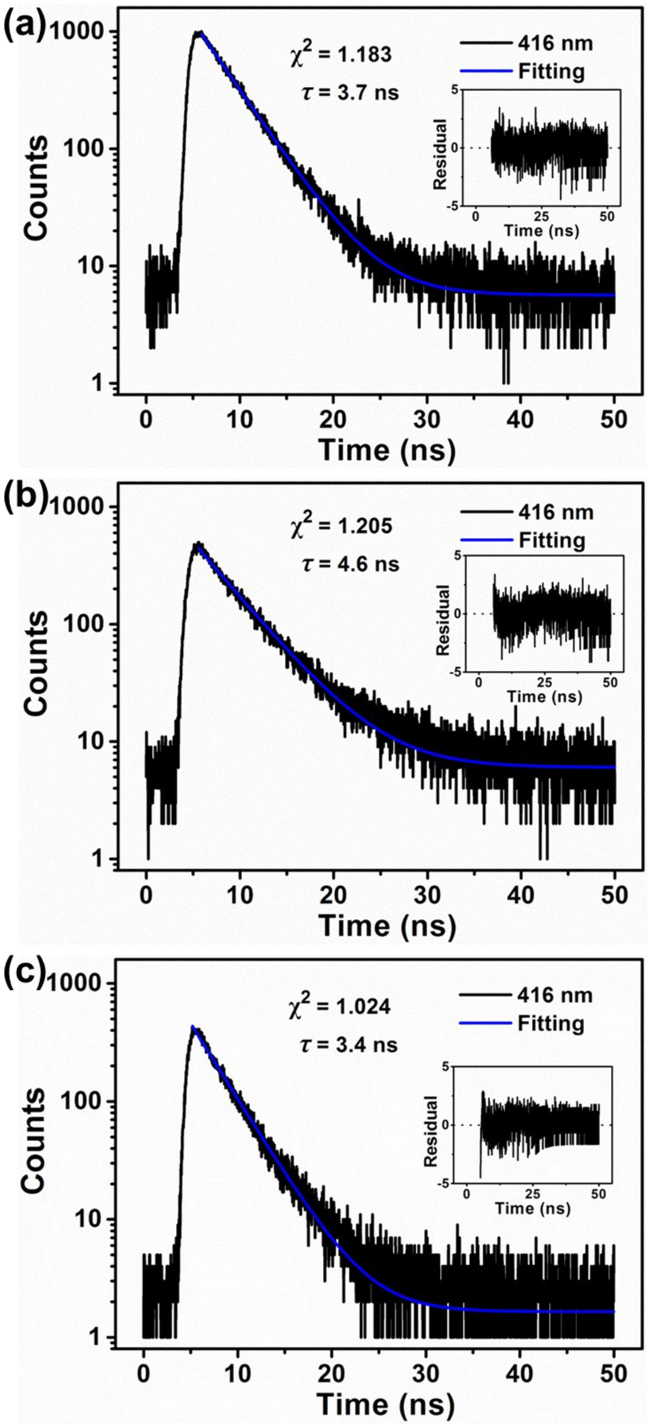

Fig. S9 Time-resolved emission decay curves monitored at 416 nm of M-CN (a), M-Me (b) and M-OMe (c) in the film states using pico-second pulsed diode laser (EPLED-340) as an excitation source. The insets are the corresponding residual-distributions. Note: Chi-square (χ^2) is a parameter to quantify the fitting quality.

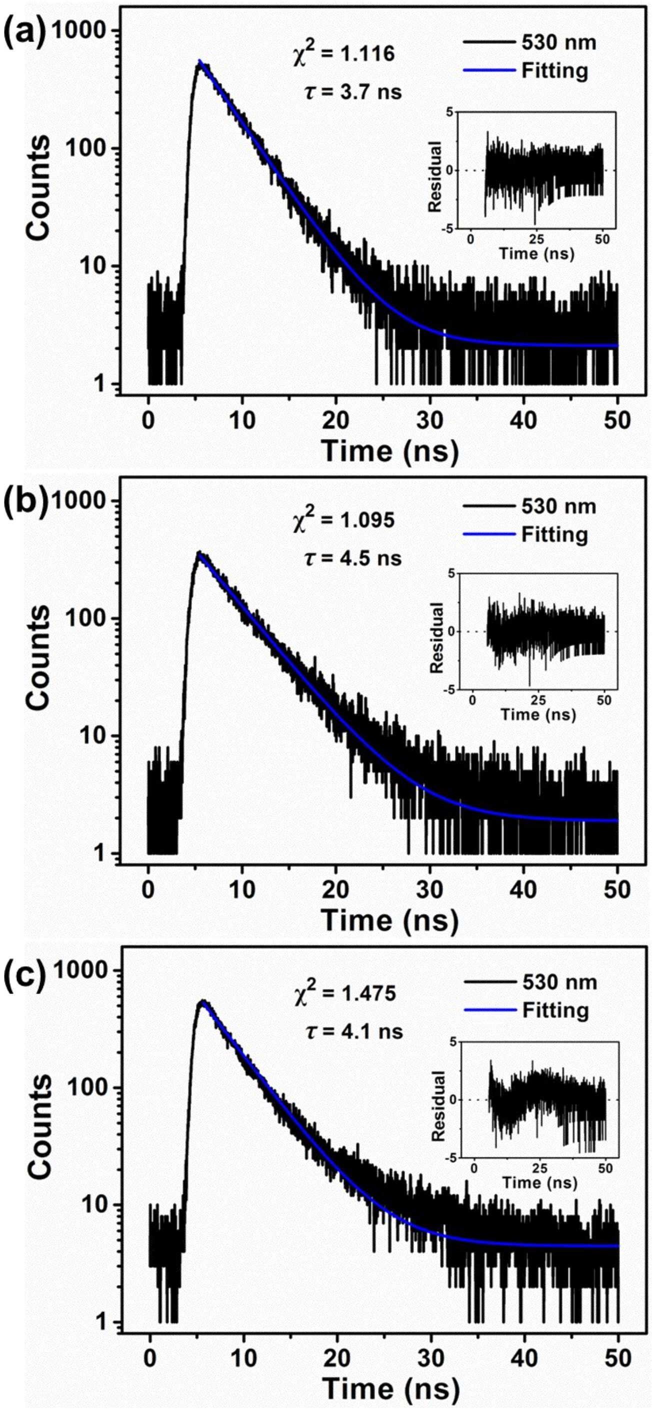

Fig. S10 Time-resolved emission decay curves monitored at 530 nm of M-CN (a), M-Me (b) and M-OMe (c) in the film states using pico-second pulsed diode laser (EPLED-340) as an excitation source. The insets are the corresponding residual-distributions. Note: Chi-square (χ^2) is a parameter to quantify the fitting quality.

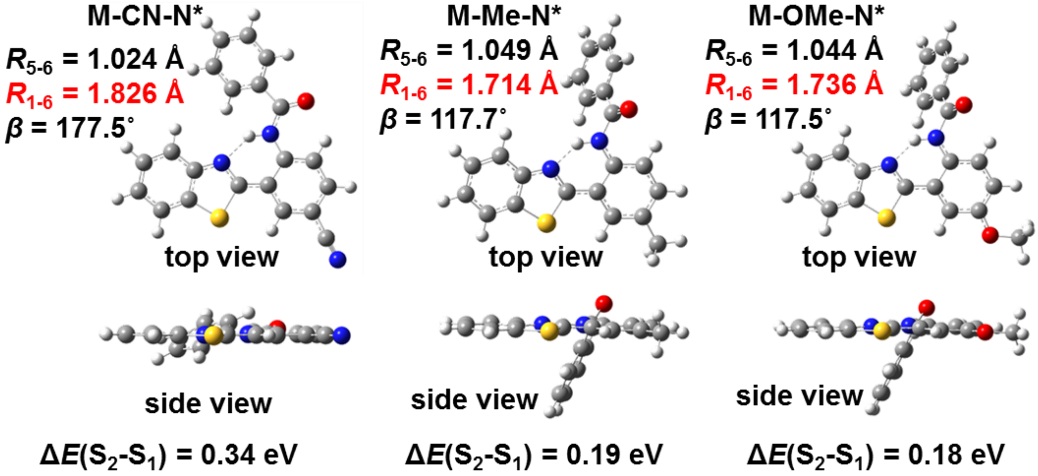

Fig. S11 Optimized S_2 geometrical structures of the three dual-fluorescence emitters with the N configuration at TD-PBE0/6-31G(d,p) level in dichloromethane.

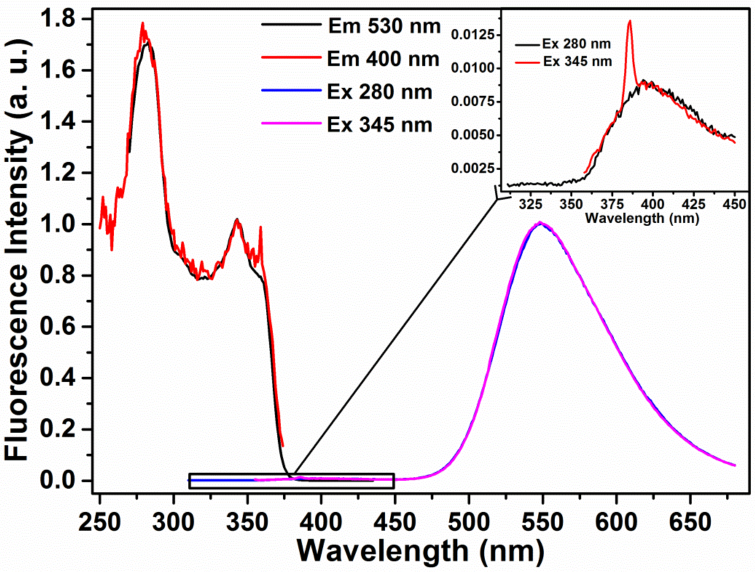

Fig. S12 Fluorescence excitation and emission spectra of M-CN in dichloromethane recorded at a concentration of 1.0×10^{-5} mol/L at ambient temperature. The detected wavelengths were set at 400 and 530 nm, and the excited wavelengths were 280 and 345 nm, respectively. The inset is an enlarged form of the N^* emission region upon excitation at 280 (black) and 345 nm (red), of which the sharp peak at 386 nm is originated from Raman scattering of the solvent.

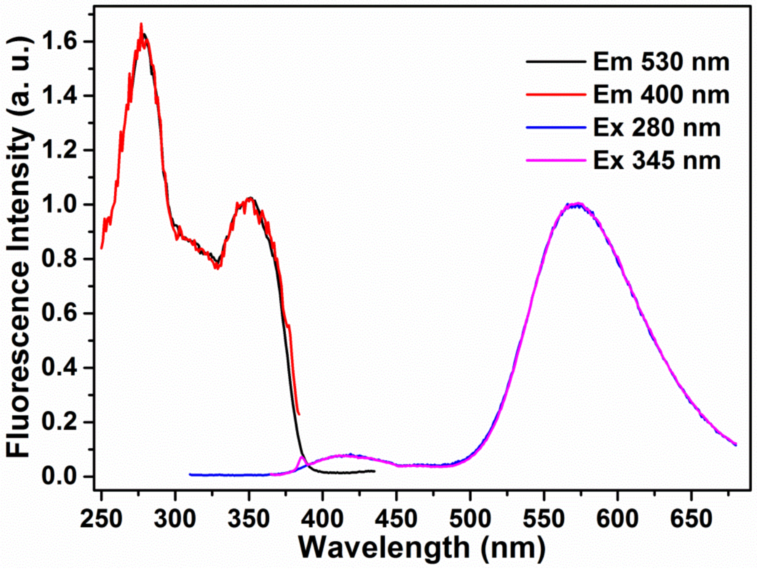

Fig. S13 Fluorescence excitation and emission spectra of M-Me in dichloromethane recorded at a concentration of 1.0×10^{-5} mol/L at ambient temperature. The detected wavelengths were set at 400 and 530 nm, and the excited wavelengths were 280 and 345 nm, respectively.

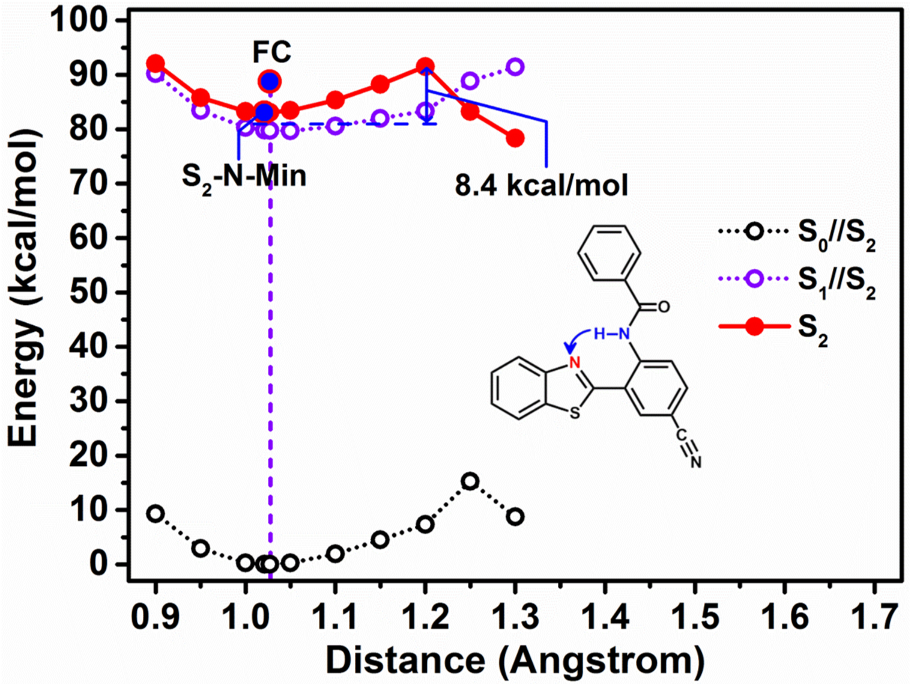

Fig. S14 Calculated S_0, S_1 and S_2 energy profiles of M-CN along with the N1-H6 distances, optimized at the ONIOM(TD-PBE0:UFF) level in the film state (S_2: the potential energy surface of the S_2 state; $S_1//S_2$: vertically projected S_1 energy on top of optimized S_2 geometries; $S_0//S_2$: vertically projected S_0 energy on top of optimized S_2 geometries). The distances are given in angstroms.

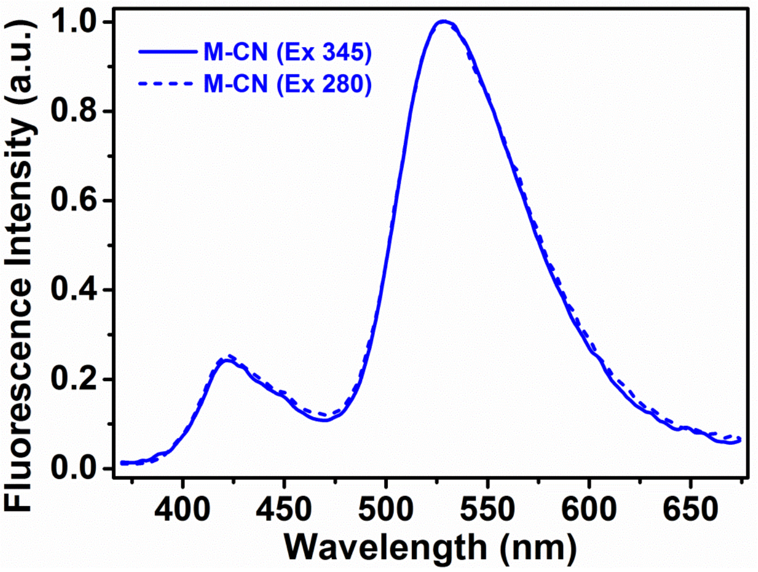

Fig. S15 Fluorescence emission spectra of M-CN in the film state at ambient temperature. The excited wavelengths were 280 (dash line) and 345 nm (solid line), respectively.

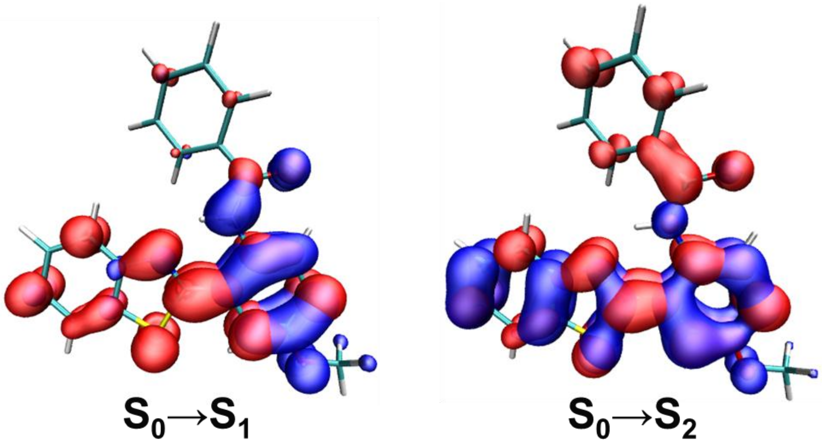

Fig. S16 Electron-hole distributions for $S_0 \rightarrow S_1$ (left) and $S_0 \rightarrow S_2$ (right) transitions of M-OMe in dichloromethane at the Franck–Condon points on the S_1 and S_2 state (red = electron, blue = hole; isovalue = 0.001).

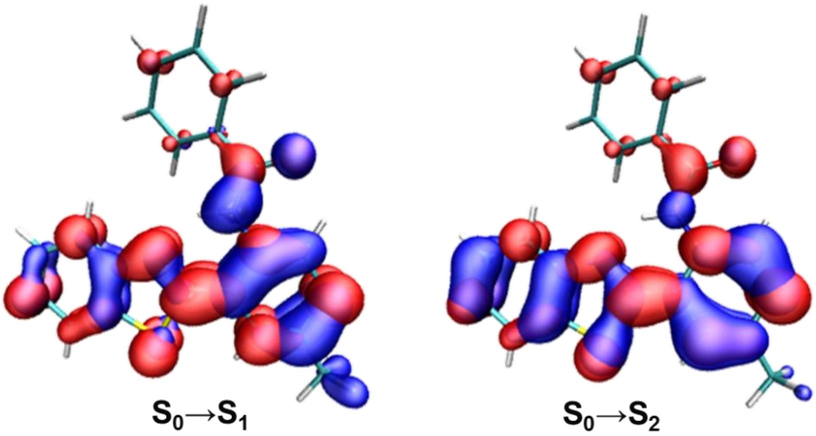

Fig. S17 Electron-hole distributions for $S_0 \rightarrow S_1$ (left) and $S_0 \rightarrow S_2$ (right) transitions of M-Me in dichloromethane at the Franck–Condon points on the S_1 and S_2 state (red = electron, blue = hole; isovalue = 0.001).

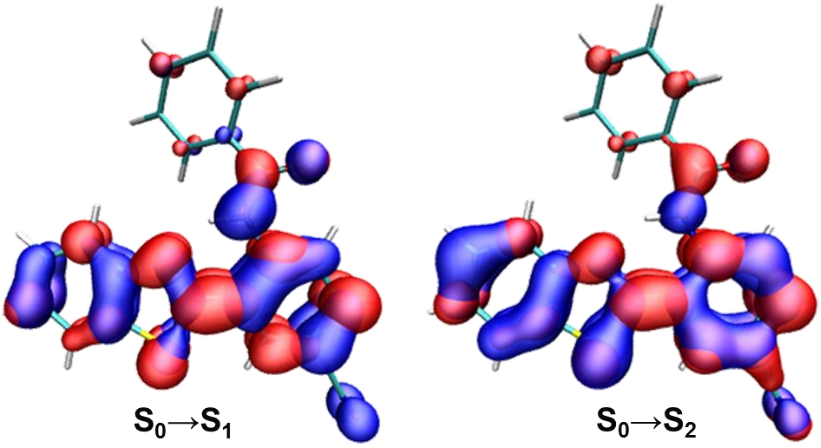

Fig. S18 Electron-hole distributions for $S_0 \rightarrow S_1$ (left) and $S_0 \rightarrow S_2$ (right) transitions of M-CN in dichloromethane at the Franck–Condon points on the S_1 and S_2 state (red = electron, blue = hole; isovalue = 0.001).

At Frank-Condon (FC) points of M-OMe in the S_1 and S_2 excited states in dichloromethane, the $S_0 \rightarrow S_1$ and $S_0 \rightarrow S_2$ transitions couple with the prominently different intramolecular charge transfer that the electron of the amide-substituted methoxyphenyl group is mainly transferred to the benzothiazole moiety during the $S_0 \rightarrow S_1$ transition, while the benzamide group gets most of the negative charge from the rest part of the molecule accompanied by the $S_0 \rightarrow S_2$ transition (Fig. S16). M-Me shows almost identical features of the $S_0 \rightarrow S_1$ and $S_0 \rightarrow S_2$ transitions (Fig. S17). These distinctive electronic transitions impart a large energy difference between the S_1 and S_2 states to M-OMe (17.3 kcal/mol, 0.75 eV at TD-PBE0/6-31G(d,p) level) and M-Me (13.4 kcal/mol, 0.58 eV at TD-PBE0/6-31G(d,p) level), as shown in Table S2. However, there are not obvious distinctions between the $S_0 \rightarrow S_1$ and $S_0 \rightarrow S_2$ transitions for M-CN (Fig. S18).

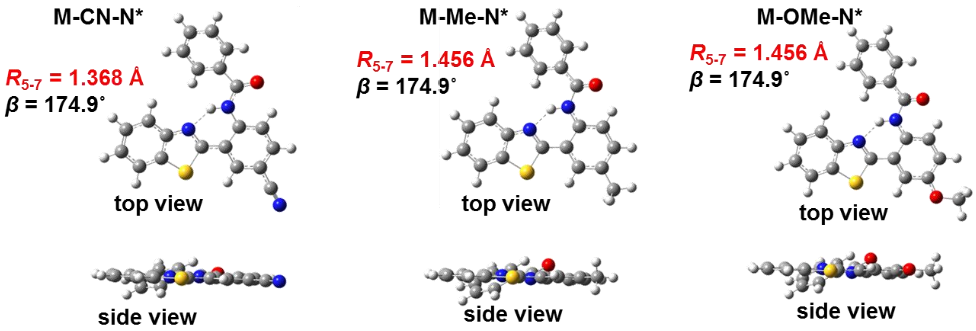

Fig. S19 Optimized S_2 geometrical structures of the three dual-fluorescence emitters in the normal form at the FC region on the S_2 state using restrained *β* dihedral angle optimization at TD-PBE0/6-31G(d,p) level in dichloromethane. The distances and the torsional angles are given in angstroms and degrees, respectively.

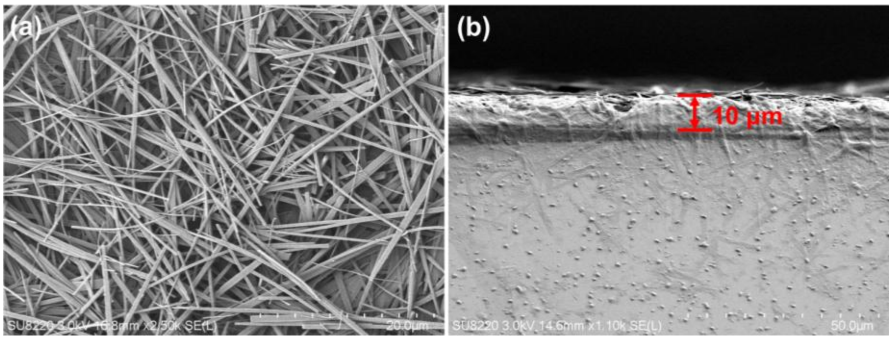

Fig. S20 Scanning electron microscopy images of the film surface (a) and side face (b) of M-CN coated on a silicon plate surface. As seen, the thickness of the film is about 10 μm. The fabrication process and the solution used for the fabrication of the film are the same with that for the spectral measurements.

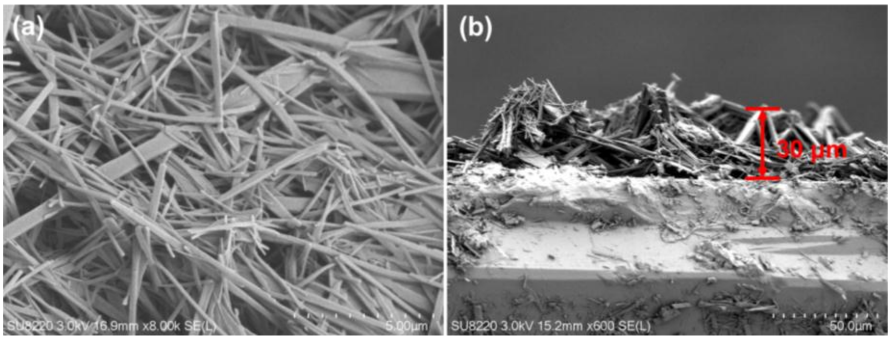

Fig. S21 Scanning electron microscopy images of the film surface (a) and side face (b) of M-Me coated on a silicon plate surface. As seen, the thickness of the film is about 30 μm. The fabrication process and the solution used for the fabrication of the film are the same with that for the spectral measurements.

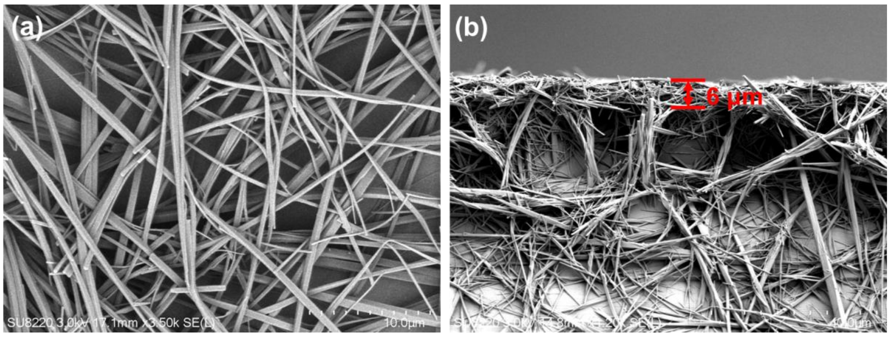

Fig. S22 Scanning electron microscopy images of the film surface (a) and side face (b) of M-OMe coated on a silicon plate surface. As seen, the thickness of the film is about 6 μm. The fabrication process and the solution used for the fabrication of the film are the same with that for the spectral measurements. It should be noted that the self-assembled structure on the side face of the film is formed from the mixed solution overflowing the silicon plate surface during the preparation process.

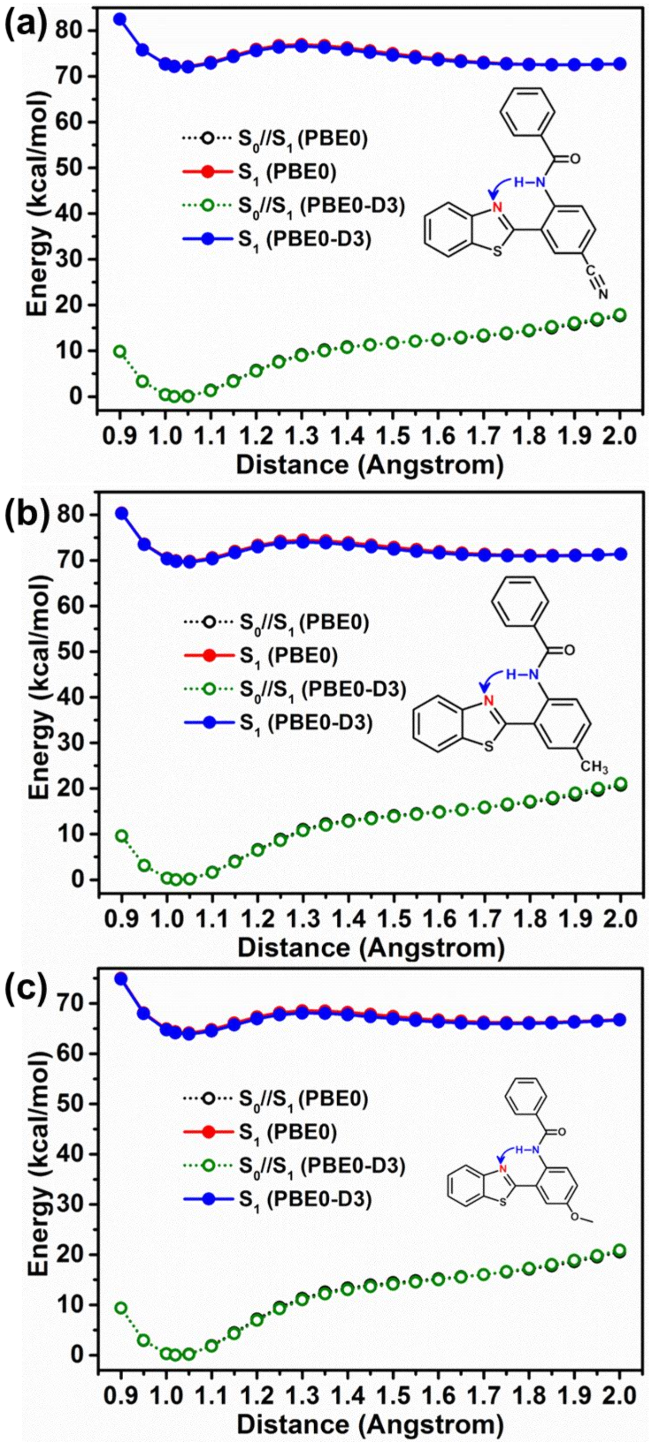

Fig. S23 Calculated S_0 and S_1 energy profiles of M-CN (a), M-Me (b) and M-OMe (c) along with the N1-H6 distances corresponding to the proton-transfer coordinates, optimized at TD-PBE0/6-31G(d,p) and TD-PBE0-D3/6-31G(d,p) levels in dichloromethane (S_1: the potential energy surface of the S_1 state; $S_0//S_1$: vertically projected S_0 energy on top of optimized S_1 geometries). The distances are given in angstroms.

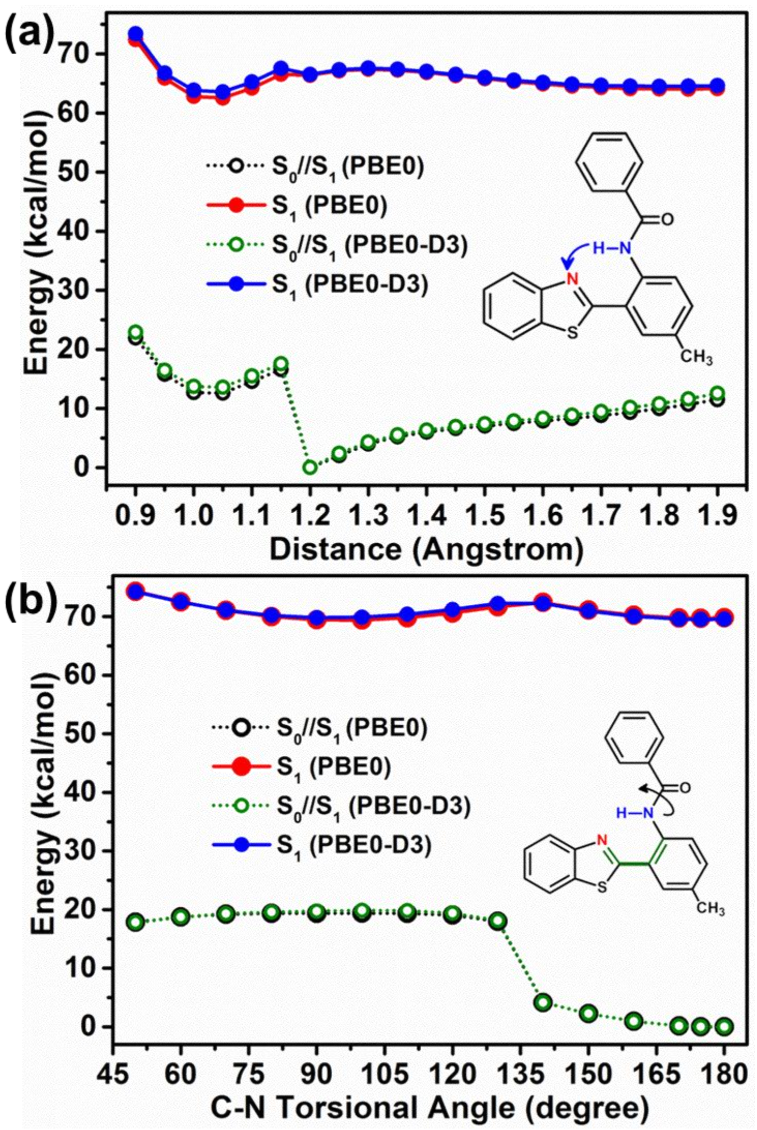

Fig. S24 Calculated S_0 and S_1 energy profiles of M-Me in the twisted configuration along with the N1-H6 distances corresponding to the proton-transfer coordinates (a) and the N5-C7 torsional coordinates (b), optimized at TD-PBE0/6-31G(d,p) and TD-PBE0-D3/6-31G(d,p) levels in dichloromethane (S_1: the potential energy surface of the S_1 state; $S_0//S_1$: vertically projected S_0 energy on top of optimized S_1 geometries). The distances and the torsional angles are given in angstroms and degrees, respectively.

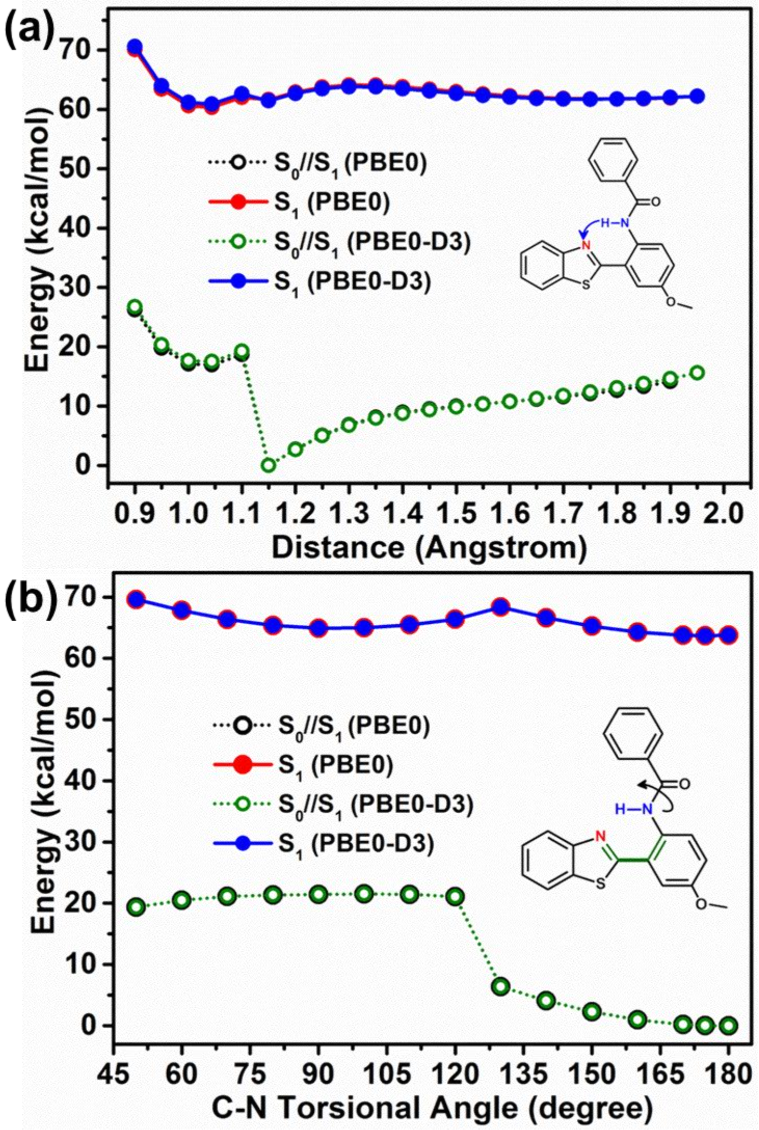

Fig. S25 Calculated S_0 and S_1 energy profiles of M-OMe in the twisted configuration along with the N1-H6 distances corresponding to the proton-transfer coordinates (a) and the N5-C7 torsional coordinates (b), optimized at TD-PBE0/6-31G(d,p) and TD-PBE0-D3/6-31G(d,p) levels in dichloromethane (S_1: the potential energy surface of the S_1 state; S_0//S_1: vertically projected S_0 energy on top of optimized S_1 geometries). The distances and the torsional angles are given in angstroms and degrees, respectively.

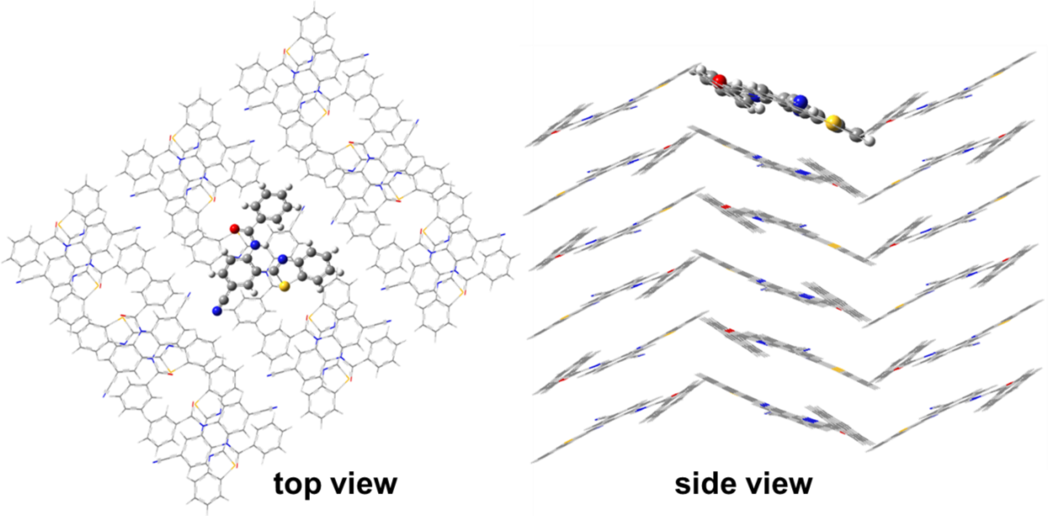

Fig. S26 Setup of our QM/MM model for a cluster with 54 M-CN molecules cut from the crystal structure with the central one as QM region.

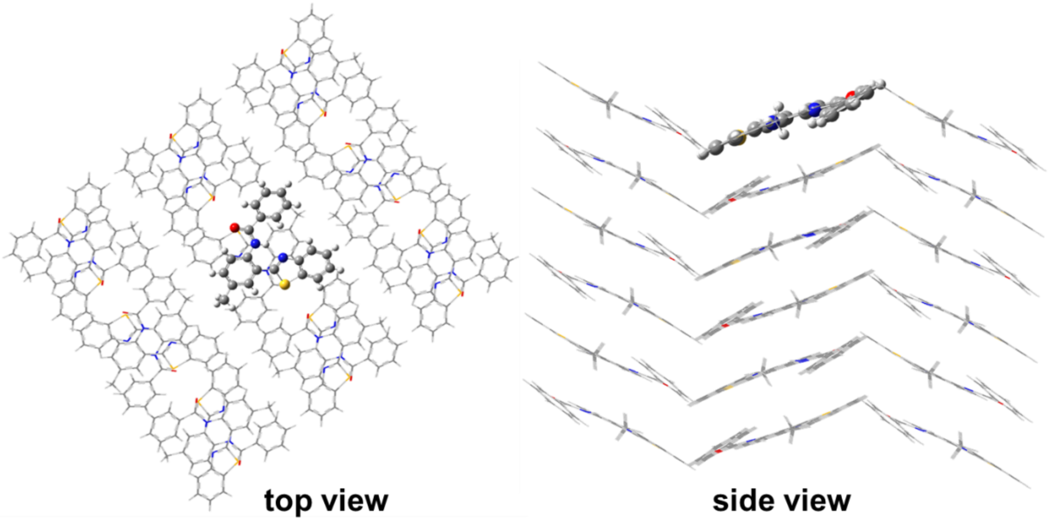

Fig. S27 Setup of our QM/MM model for a cluster with 54 M-Me molecules cut from the crystal structure with the central one as QM region.

.

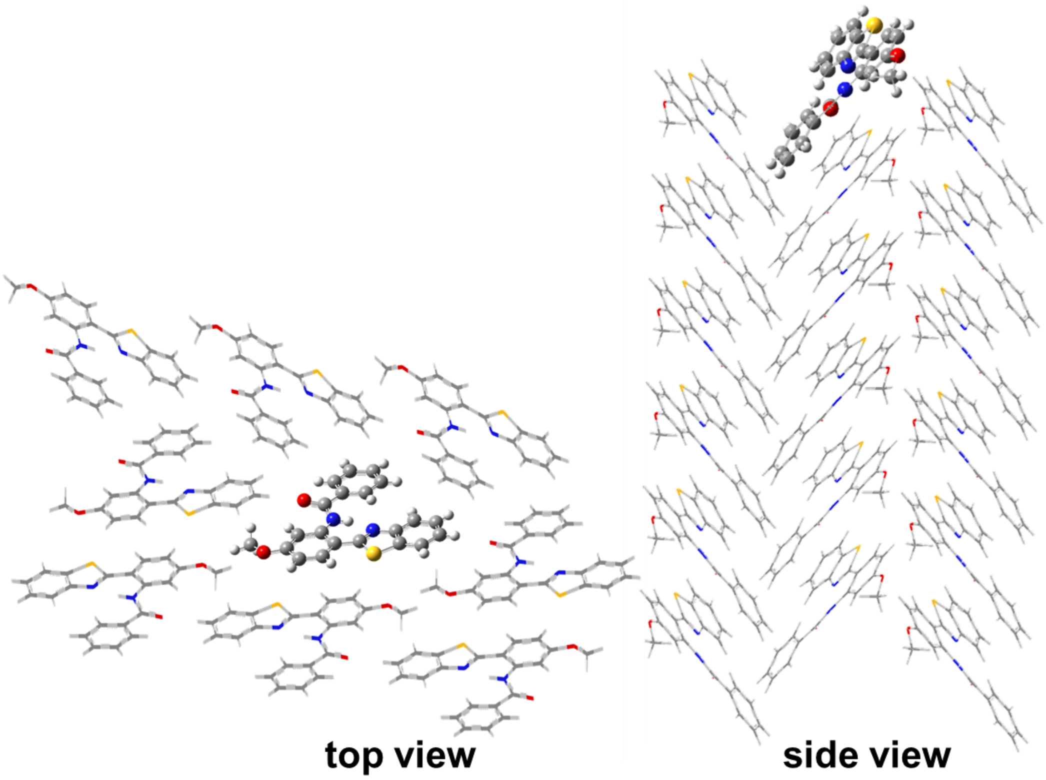

Fig. S28 Setup of our QM/MM model for a cluster with 54 M-OMe molecules cut from the crystal structure with the central one as QM region.

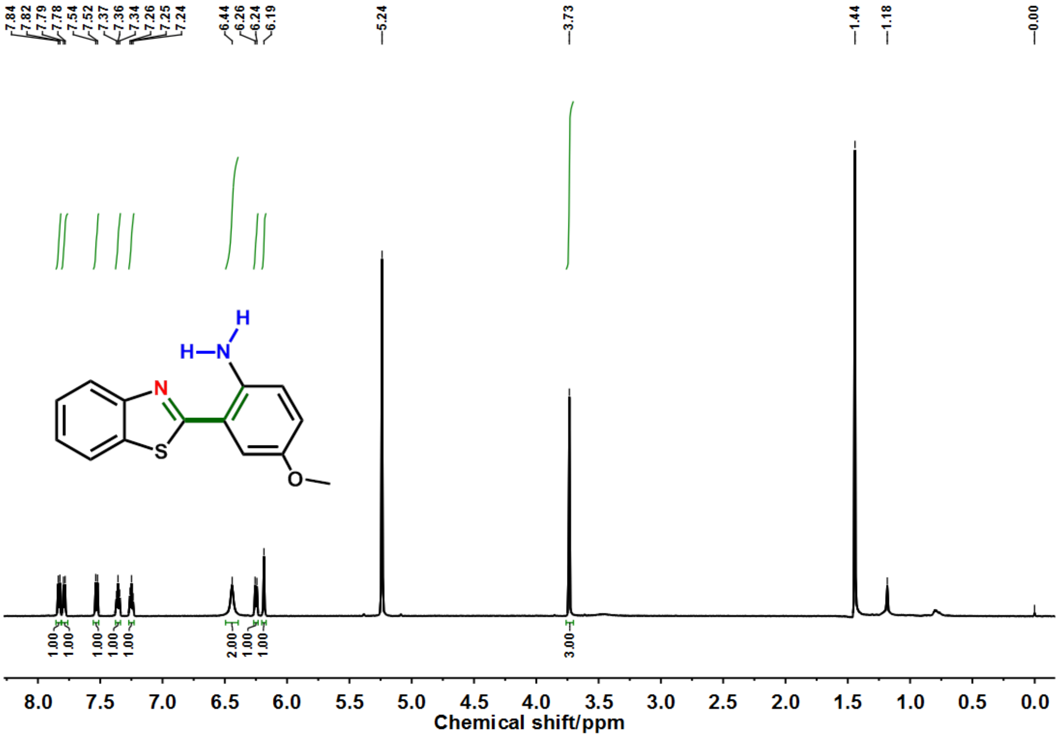

Fig. S29 ^{1}H NMR spectrum of M-OMe-NH$_2$ in deuterated dichloromethane.

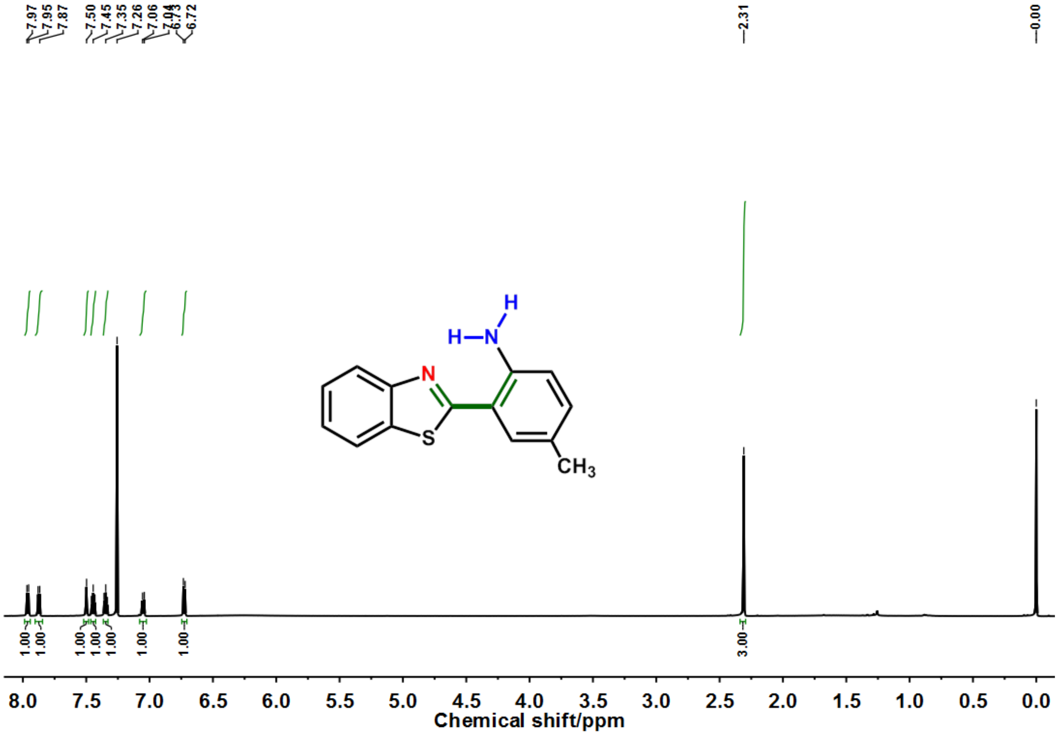

Fig. S30 ^{1}H NMR spectrum of M-Me-NH$_2$ in deuterated chloroform.

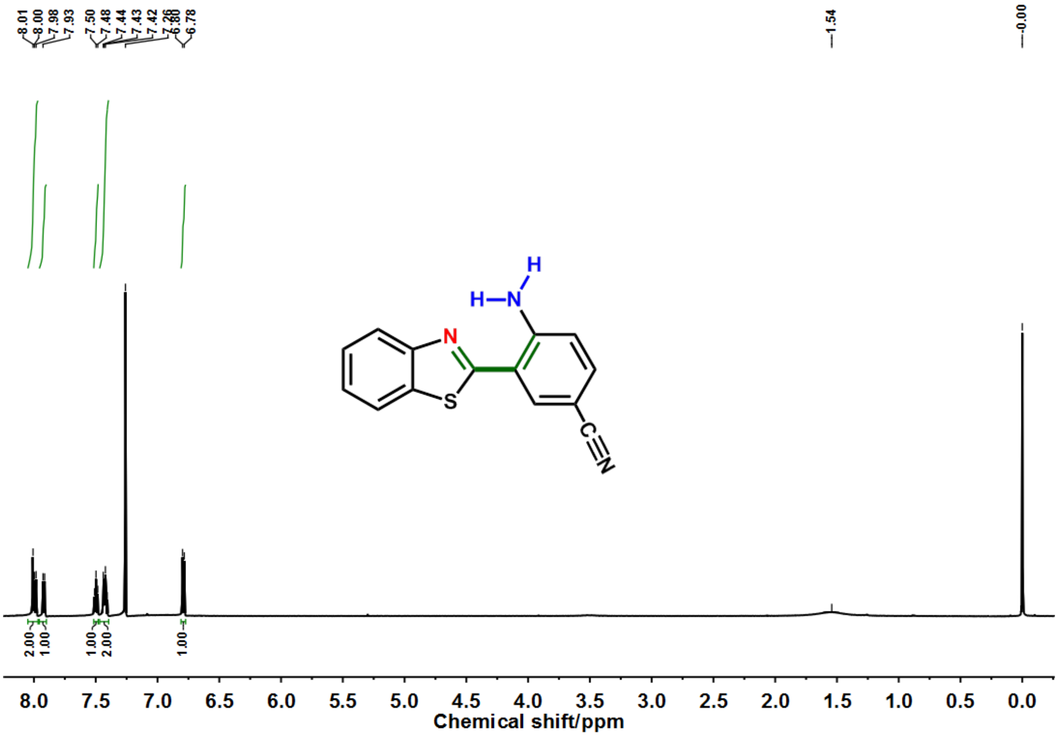

Fig. S31 ^{1}H NMR spectrum of M-CN-NH$_2$ in deuterated chloroform.

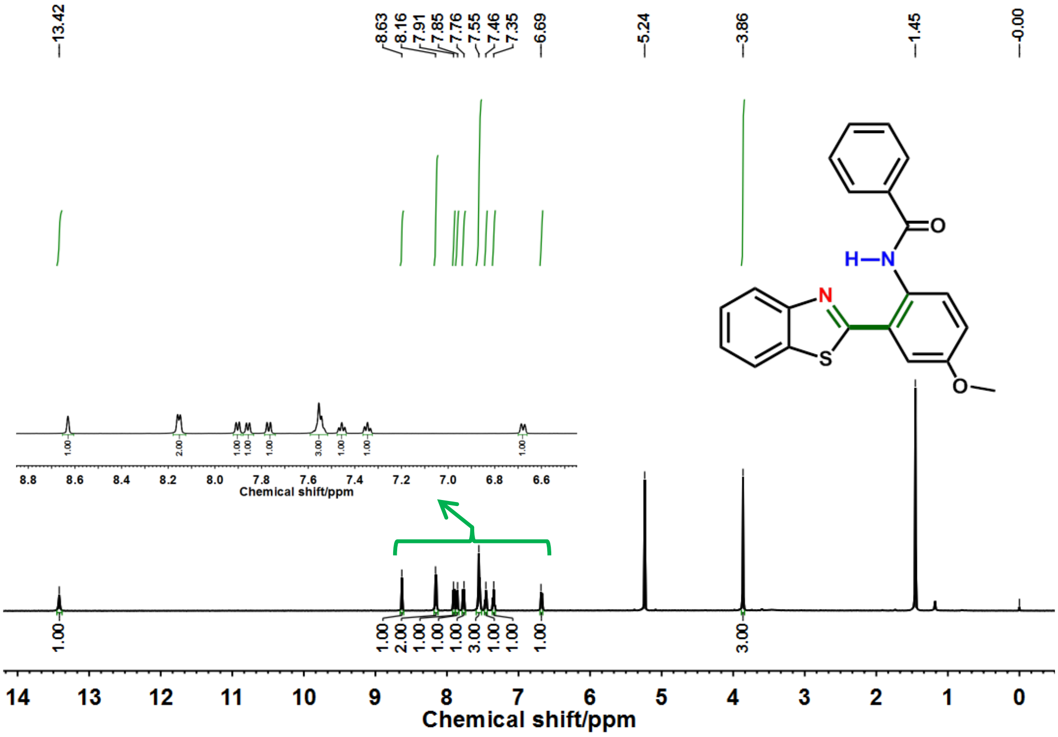

Fig. S32 ^{1}H NMR spectrum of M-OMe in deuterated dichloromethane.

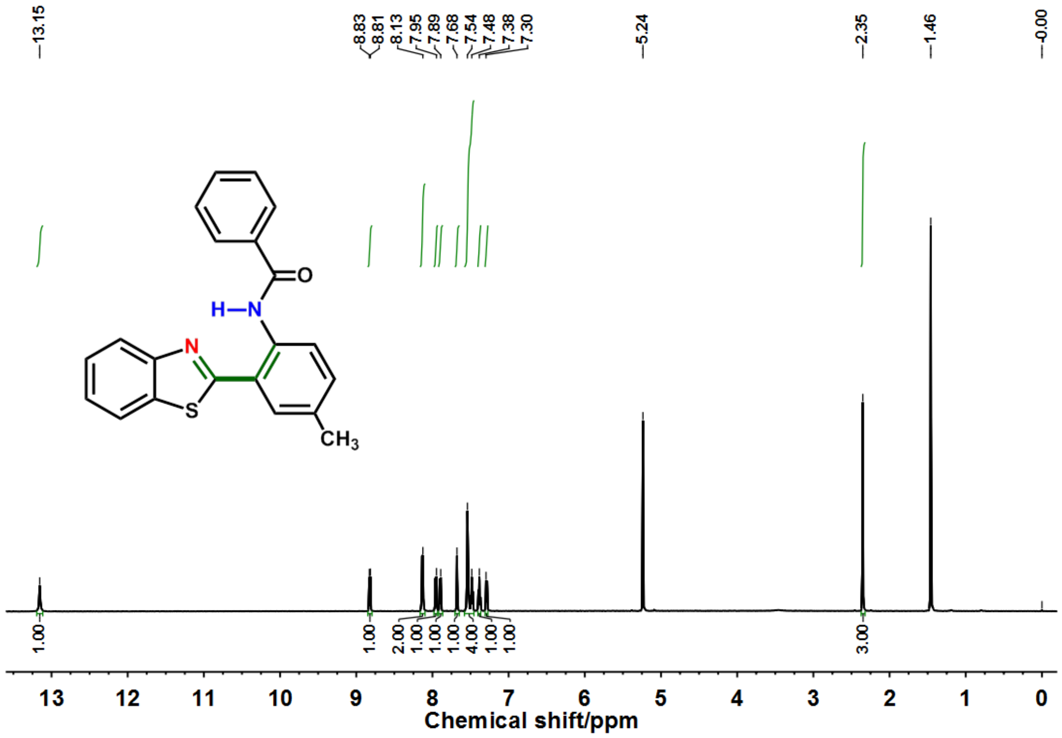

Fig. S33 ^{1}H NMR spectrum of M-Me in deuterated dichloromethane.

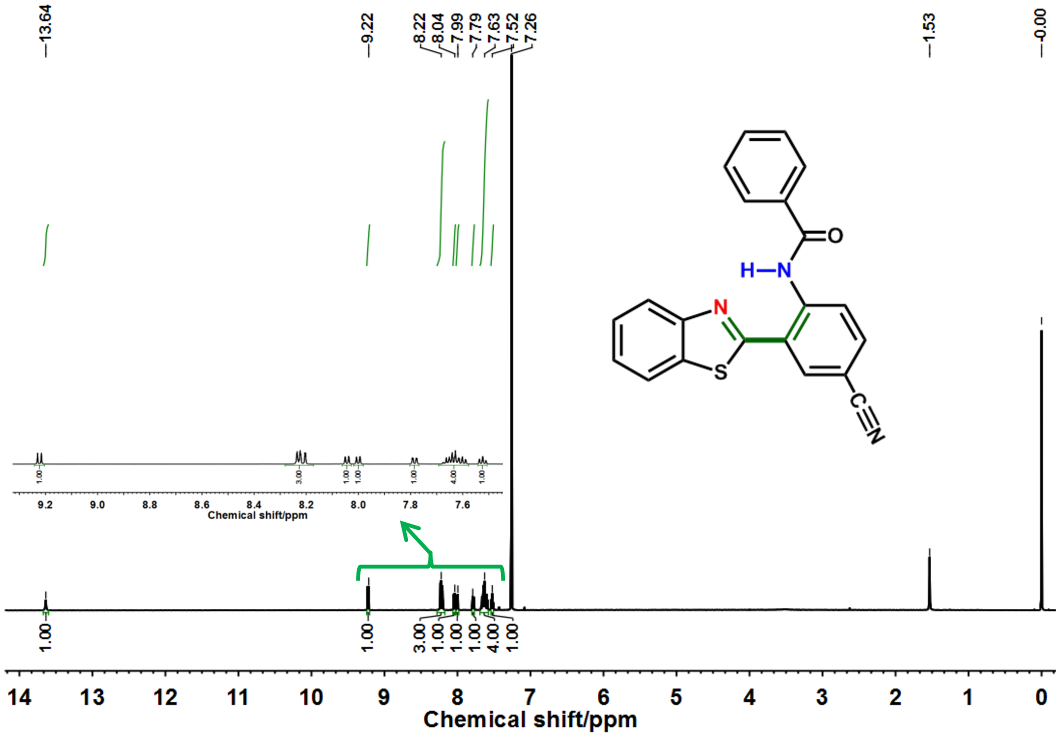

Fig. S34 ^{1}H NMR spectrum of M-CN in deuterated chloroform.

Table S6. Crystallographic refinement data of M-OMe.

Crystal data	**M-OMe**	
Formula	$C_{21}H_{16}N_2O_2S$	
Formula weight	360.42	
Temperature	193 K	
Wavelength	1.34139 Å	
Crystal system	Orthorhombic	
Space group	$Pna2_1$	
Unit cell dimensions	a = 27.4596(18) Å	alpha = 90 °
	b = 11.0411(7) Å	beta = 90 °
	c = 5.5352(4) Å	gamma = 90 °
	Volume = 1678.2(2) $Å^3$	
Z	4	
Density (calculated)	1.427 g/cm^3	
Absorption coefficient	1.218 mm^{-1}	
F(000)	752	
Crystal size	0.12 × 0.1 × 0.1 mm^3	
2Θ range for data collection	5.6 to 121.154 °	
Index ranges	$-35 \leq h \leq 35$, $-14 \leq k \leq 13$, $-7 \leq l \leq 4$	
Reflections collected	16088	
Independent reflections	3191 [R(int) = 0.0573]	
Absorption correction type	Multi-scan	
Max. and min. transmission	0.752 and 0.625	
Data / restraints / parameters	3191 / 1/ 236	
Goodness-of-fit on F^2	1.073	
Final R indexes [I>=2σ (I)]	R1 = 0.0285, wR2 = 0.0714	
Final R indexes [all data]	R1 = 0.0329, wR2 = 0.0739	
Largest diff. peak and hole	0.16 and -0.24 e.$Å^{-3}$	
CCDC Number	2101306	

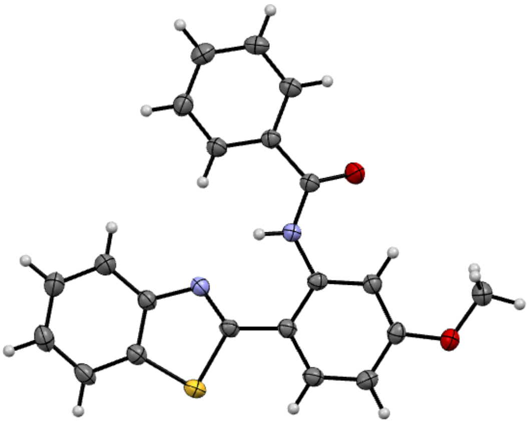

Fig. S35 Crystal structure of 50% probability density ellipsoids of M-OMe.

Table S7. Crystallographic refinement data of M-Me.

Crystal data	**M-Me**	
Formula	$C_{21}H_{16}N_2OS$	
Formula weight	344.42	
Temperature	193 K	
Wavelength	1.34139 Å	
Crystal system	Monoclinic	
Space group	$P2_1/c$	
Unit cell dimensions	a = 12.0592(8) Å	alpha = 90 °
	b = 18.9863(12) Å	beta = 103.779(3) °
	c = 7.3256(5)	gamma = 90 °
	Volume = 1629.00(19) $Å^3$	
Z	4	
Density (calculated)	1.404 g/cm^3	
Absorption coefficient	1.207 mm^{-1}	
F(000)	720	
Crystal size	0.12 × 0.1 × 0.1 mm^3	
2Θ range for data collection	7.716 to 126.654	
Index ranges	$-9 \leq h \leq 15$, $-24 \leq k \leq 22$, $-9 \leq l \leq 9$	
Reflections collected	13065	
Independent reflections	3901 [R(int) = 0.0567]	
Absorption correction type	Multi-scan	
Max. and min. transmission	0.752 and 0.554	
Data / restraints / parameters	3901 / 0/ 227	
Goodness-of-fit on F^2	1.047	
Final R indexes [$I>=2\sigma(I)$]	R1 = 0.0458, wR2 = 0.1158	
Final R indexes [all data]	R1 = 0.0615, wR2 = 0.1264	
Largest diff. peak and hole	0.32 and -0.47 e.$Å^{-3}$	
CCDC Number	2101308	

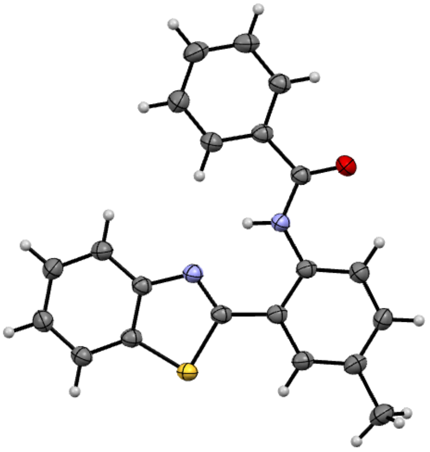

Fig. S36 Crystal structure of 50% probability density ellipsoids of M-Me.

Table S8. Crystallographic refinement data of M-CN.

Crystal data	**M-CN**	
Formula	C21H13N3OS	
Formula weight	355.40	
Temperature	296.15 K	
Wavelength	0.71073 Å	
Crystal system	Monoclinic	
Space group	$P2_1/c$	
Unit cell dimensions	a = 12.5048(7) Å	alpha = 90 °
	b = 18.8823(10) Å	beta = 106.626(2)
	c = 7.2768(4) Å	gamma = 90 °
	Volume = 1646.36(16) Å^3	
Z	4	
Density (calculated)	1.434 g/cm^3	
Absorption coefficient	0.212 mm^{-1}	
F(000)	736	
Crystal size	0.12 × 0.1 × 0.1 mm^3	
2Θ range for data collection	4.026 to 55.068 °	
Index ranges	$-16 \leq h \leq 15$, $-24 \leq k \leq 24$, $-9 \leq l \leq 9$	
Reflections collected	15162	
Independent reflections	3788 [R(int) = 0.0814]	
Absorption correction type	Multi-scan	
Max. and min. transmission	0.746 and 0.668	
Data / restraints / parameters	3788 / 0/ 235	
Goodness-of-fit on F^2	1.057	
Final R indexes [I>=2σ (I)]	R1 = 0.0466, wR2 = 0.1144	
Final R indexes [all data]	R1 = 0.0607, wR2 = 0.1256	
Largest diff. peak and hole	0.31 and -0.28 e.Å^{-3}	
CCDC Number	2101307	

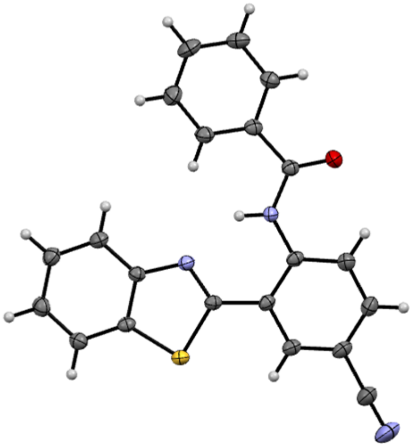

Fig. S37 Crystal structure of 50% probability density ellipsoids of M-CN.

Part V. Cartesian coordinates

Cartesian coordinates of important geometries of the N-H-type ESIPT molecules in dichloromethane optimized at (TD)-PBE0/6-31G(d,p) level of theory

S_0-min-M-CN-N (the S_0 minimum of M-CN in the normal form)

Energy: -1444.45092616

C	-5.22983800	-2.06397000	-0.43936300
C	-5.49820200	-0.83945300	0.17086800
C	-4.45871100	-0.09411400	0.72286700
C	-3.15001900	-0.56204200	0.65399500
C	-2.87486800	-1.78579500	0.03317300
C	-3.92562600	-2.53873000	-0.49982800
C	-1.50100500	-2.36693000	-0.06078000
C	0.87843700	-1.65398200	0.00354900
C	1.75226100	-0.52428100	0.00426700
C	3.13076700	-0.74405600	0.02552900
C	3.66570100	-2.02976200	0.04741100
C	2.80112400	-3.13382600	0.04707600
C	1.43404200	-2.94610900	0.02454500
C	1.25684900	0.85370700	-0.01980700
C	-0.19105500	2.54522100	-0.07697800
C	-1.43061200	3.19431700	-0.12008400
C	-1.45330100	4.57921300	-0.13905400
C	-0.26257600	5.32181000	-0.11617900
C	0.97597600	4.69528300	-0.07522900
C	0.99876600	3.30165600	-0.05664100
N	-0.48606500	-1.43988600	-0.00208800
N	-0.00389700	1.18226200	-0.05363600
O	-1.32797600	-3.57212800	-0.19338600
S	2.36457300	2.22849000	-0.00929800
H	-6.03891700	-2.64884600	-0.86621200
H	-6.51800200	-0.46980400	0.22281400
H	-4.66686700	0.85026400	1.21666100
H	-2.35518700	0.01911000	1.11283200
H	-3.69820100	-3.49397000	-0.96190100
H	3.81226500	0.10051600	0.02499400
H	3.20738800	-4.13938100	0.06389200
H	0.76227100	-3.79230000	0.01623400
H	-2.34414000	2.60868700	-0.14038300
H	-2.40541600	5.09926100	-0.17270100
H	-0.30776500	6.40627200	-0.13146900
H	1.89350300	5.27359400	-0.05888600
H	-0.73932700	-0.44560200	-0.03376100
C	5.08053800	-2.21567600	0.06876600
N	6.23241100	-2.37116300	0.08645700

S_1-min-M-CN-N (the S_1 minimum of M-CN in the normal form)

Energy: -1444.32711135

C	-5.20627100	-2.17409100	-0.31099100	N	-0.44062300	-1.44949400	-0.02022900
C	-5.47185500	-0.90821500	0.21371000	N	-0.05396300	1.17797500	-0.03889000
C	-4.42151400	-0.10250500	0.65037800	O	-1.26786800	-3.58299400	-0.26906600
C	-3.10855300	-0.54809800	0.55203000	S	2.34013400	2.28236300	0.00789800
C	-2.83403300	-1.81666000	0.01660700	H	-6.02261900	-2.80568200	-0.64793500
C	-3.89893100	-2.62855500	-0.40116400	H	-6.49546900	-0.55350200	0.28767600
C	-1.47152500	-2.38524200	-0.09974900	H	-4.62591800	0.87474400	1.07729900
C	0.90213100	-1.65640600	-0.01029200	H	-2.30998100	0.08911200	0.92115900
C	1.76689500	-0.45760100	0.01238000	H	-3.67382300	-3.61270700	-0.79868600
C	3.16684000	-0.68468000	0.04448600	H	3.84534100	0.16117400	0.06262700
C	3.69226700	-1.96405400	0.05330900	H	3.28242900	-4.10106900	0.03596200
C	2.84818400	-3.10849900	0.02854400	H	0.81825800	-3.79384800	-0.02850200
C	1.48063800	-2.94050700	-0.00359800	H	-2.41315000	2.55721200	-0.16841500
C	1.25847500	0.85292300	-0.00332300	H	-2.50736600	5.03901500	-0.20064000
C	-0.25066600	2.50499000	-0.07492000	H	-0.43275900	6.38683200	-0.14202900
C	-1.50793000	3.15439300	-0.13418300	H	1.79169500	5.29090600	-0.05204900
C	-1.54792700	4.53273900	-0.15515100	H	-0.68977600	-0.44047400	-0.03628700
C	-0.36653100	5.30371500	-0.12306200	C	5.10728600	-2.14008100	0.08775900
C	0.88553200	4.69466400	-0.07241900	N	6.25947800	-2.29472600	0.11600600
C	0.94077000	3.30812700	-0.05072100				

S_1-min-M-CN-T (the S_1 minimum of M-CN in the phototautomeric form)

Energy: -1444.32649827

C	-5.37435700	-1.83342600	-0.20377200	N	-0.58566200	-1.29072800	-0.02690400
C	-5.54668700	-0.69550900	0.58547700	N	0.11634000	1.26622900	-0.28358500
C	-4.43449200	-0.01615900	1.07997600	O	-1.50165400	-3.22532200	-0.93118900
C	-3.15314300	-0.46504800	0.77872900	S	2.49928400	2.06574500	0.21629000
C	-2.97216200	-1.60259200	-0.01907000	H	-6.24023200	-2.36509200	-0.58718300
C	-4.09552800	-2.28727700	-0.49854100	H	-6.54696600	-0.34129500	0.81720000
C	-1.62216400	-2.13794800	-0.35934200	H	-4.56610900	0.86324300	1.70334400
C	0.70660200	-1.68798700	-0.01769100	H	-2.28680700	0.05249900	1.17778500
C	1.71031600	-0.62564500	-0.00148500	H	-3.94011700	-3.17316900	-1.10584000
C	3.05199500	-0.99188900	0.02689700	H	3.82824700	-0.23471400	-0.01694800
C	3.44456400	-2.35064300	0.10547300	H	2.79655100	-4.40632000	0.17888000
C	2.49114900	-3.36842700	0.11510400	H	0.38905800	-3.80596400	0.05699400
C	1.14187300	-3.02990600	0.04534600	H	-2.11312900	2.89515000	-0.64009300
C	1.35636800	0.76446900	-0.03055300	H	-1.94228000	5.37145300	-0.53276200
C	-0.00296200	2.62356700	-0.25390500	H	0.22701800	6.47452800	-0.09467900
C	-1.16306300	3.38274600	-0.44862000	H	2.28246300	5.12392100	0.25723900
C	-1.05419900	4.76482700	-0.38543200	H	-0.63619300	0.56836600	-0.33287200
C	0.17347400	5.39169000	-0.13656300	C	4.83048300	-2.66894900	0.17244700
C	1.33120500	4.64093000	0.06037300	N	5.96397600	-2.92622300	0.22697700
C	1.23249200	3.25702600	0.00055100				

S_2-min-M-CN-N (the S_2 minimum of M-CN in the normal form)

Energy: -1444.30736913

C	1.70733600	0.58740800	-0.01488500	C	4.97144300	2.42527200	-0.05464800
C	-0.06620000	-2.55261200	0.05483900	N	6.11752400	2.62423700	-0.06641100
C	1.16643400	-3.24575000	0.05439000	N	-0.56877400	1.44390300	-0.01228100
C	-2.96870800	1.67604300	-0.03079800	N	0.00668600	-1.20242300	0.01729800
C	-1.62002100	2.31684800	0.04905700	S	2.47190400	-2.12340400	0.01294500
C	0.79314600	1.71564500	-0.01204900	O	-1.50483100	3.53590300	0.17266600
C	1.27335600	-0.75634700	0.00176000	H	3.81854100	0.07498700	-0.03158500
C	3.09406100	0.88314400	-0.02920900	H	-2.20276400	-2.81451000	0.11506300
C	-1.23936100	-3.31354000	0.09972300	H	-3.86358000	3.38208700	0.90042200
C	3.56352200	2.18897300	-0.04038900	H	2.19482000	-5.14941400	0.07775900
C	-4.05291800	2.40283500	0.47267400	H	-0.78320000	0.44333300	0.01132500
C	1.23386300	-4.64562100	0.08533700	H	0.58864900	3.83274700	-0.01214700
C	1.29807300	3.01695800	-0.02200700	H	0.08325900	-6.48302200	0.14921600
C	-3.19755700	0.42191400	-0.61071300	H	3.03307800	4.29172500	-0.04503300
C	-1.17271400	-4.74129300	0.13167700	H	-2.37961000	-0.14401100	-1.04799100
C	0.03444700	-5.40146100	0.12528500	H	-2.10242600	-5.29880300	0.16210500
C	-4.48669200	-0.09928500	-0.66559000	H	-4.65588900	-1.06732700	-1.12807900
C	2.66437800	3.27304500	-0.03680300	H	-6.17022500	2.44478200	0.82949700
C	-5.33769600	1.87638600	0.42547500	H	-6.56244500	0.21146200	-0.18430900
C	-5.55786900	0.62196700	-0.14228100				

S$_0$-min-M-Me-N (the S$_0$ minimum of M-Me in the normal form)

Energy: -1391.58166836

C	-5.50442800	-0.42789500	-0.44702600	N	0.48653900	1.03152000	-0.04726100
C	-5.38080800	0.82563500	0.15051500	O	-2.27065900	-3.07477900	-0.17075400
C	-4.16147300	1.21654600	0.69935300	S	3.06632500	1.26809900	-0.00881700
C	-3.06280000	0.36414600	0.64071800	H	-6.45466500	-0.73760300	-0.87165600
C	-3.17908700	-0.89079100	0.03246900	H	-6.23566900	1.49399100	0.19504800
C	-4.41136700	-1.28438500	-0.49756400	H	-4.06625500	2.18411700	1.18310200
C	-2.05137800	-1.87291800	-0.05067600	H	-2.12663000	0.67437900	1.09629700
C	0.43470300	-1.94088400	0.01017700	H	-4.49078300	-2.26824600	-0.94869900
C	1.61423700	-1.14643200	0.00970000	H	3.76501000	-1.18811300	0.03028100
C	2.86111100	-1.79284200	0.03156400	H	1.88323600	-5.01617800	0.07357200
C	2.99718000	-3.17265100	0.05496800	H	-0.32934600	-3.93877500	0.02738300
C	1.81976000	-3.93090000	0.05557700	H	-1.27470800	3.12988700	-0.13103700
C	0.56904000	-3.33776500	0.03308500	H	-0.54044400	5.51036000	-0.16762600
C	1.57572500	0.31430400	-0.01531500	H	1.86479800	6.08186000	-0.13329200
C	0.74523900	2.38285800	-0.07201500	H	3.58998400	4.30533100	-0.06291700
C	-0.22199200	3.39381400	-0.11368500	H	-0.73702000	-0.28888200	-0.02862100
C	0.19709900	4.71454800	-0.13503600	C	4.34619300	-3.83233500	0.07696500
C	1.56182800	5.03956000	-0.11606300	H	4.48665000	-4.47417800	-0.79935400
C	2.53565500	4.04975600	-0.07627500	H	5.15206900	-3.09440000	0.08565400
C	2.11401100	2.72144800	-0.05524600	H	4.46107500	-4.46759200	0.96166700
N	-0.80566800	-1.31069300	0.00442800				

S_1-min-M-Me-N (the S_1 minimum of M-Me in the normal form)

Energy: -1391.46223686

C	-5.47335600	-0.73849200	-0.27728000
C	-5.36900000	0.55999200	0.22519100
C	-4.12766100	1.04915000	0.62992600
C	-2.99137600	0.25620900	0.52277800
C	-3.08731800	-1.04819100	0.00877900
C	-4.34516300	-1.53844700	-0.37736900
C	-1.94045300	-1.97200100	-0.11675700
C	0.54416000	-1.93394300	-0.00862900
C	1.70634300	-1.02887900	0.01976700
C	2.97552400	-1.63884600	0.05887700
C	3.15558500	-3.01661800	0.07416500
C	2.01582600	-3.86404900	0.04695200
C	0.74637200	-3.33304800	0.00582300
C	1.57431500	0.38260300	0.00236800
C	0.56998400	2.38545400	-0.07798400
C	-0.46135200	3.34987800	-0.14658300
C	-0.12759400	4.69156900	-0.16720700
C	1.21251100	5.11451600	-0.12638800
C	2.25061500	4.18470200	-0.06641100
C	1.92656500	2.83524100	-0.04481600
N	-0.68677800	-1.36256400	-0.02861700
N	0.40270700	1.04898700	-0.04163200
O	-2.07730400	-3.17898600	-0.29949300
S	2.99660600	1.46182300	0.02179200
H	-6.43897200	-1.12488400	-0.58949200
H	-6.25284200	1.18553900	0.30641800
H	-4.04482000	2.05174900	1.03887900
H	-2.04094700	0.65482700	0.86604600
H	-4.40889300	-2.55228900	-0.75860700
H	3.85859600	-1.00621400	0.07844600
H	2.15031700	-4.94113900	0.05948400
H	-0.12784400	-3.96803100	-0.02117200
H	-1.49526600	3.02210000	-0.18873900
H	-0.91694700	5.43583200	-0.21983600
H	1.44452600	6.17464800	-0.14570500
H	3.28541900	4.51093700	-0.03946900
H	-0.63834000	-0.32075800	-0.04614500
C	4.52234900	-3.61583900	0.11724100
H	4.68852600	-4.25760900	-0.75626200
H	5.30402000	-2.85422300	0.14185300
H	4.63344400	-4.25850200	0.99864500

S_1-min-M-Me-T (the S_1 minimum of M-Me in the phototautomeric form)

Energy: -1391.46015564

C	-5.52038200	-0.31497200	-0.28654300	N	0.56255300	1.04639400	-0.23533500
C	-5.36864400	0.85758900	0.45415900	O	-2.24683400	-2.86959500	-0.72955000
C	-4.12015900	1.19110600	0.97739000	S	3.08609800	1.20442100	0.18098900
C	-3.02536700	0.36343700	0.75129200	H	-6.49263400	-0.57919900	-0.69248600
C	-3.16691400	-0.81142000	0.00095700	H	-6.22209800	1.50695500	0.62677200
C	-4.42899300	-1.14624700	-0.50478300	H	-4.00052400	2.09576500	1.56648100
C	-2.02890200	-1.74449300	-0.26059000	H	-2.05854400	0.61180900	1.17735800
C	0.34646700	-1.93939600	0.01745800	H	-4.52820400	-2.06587400	-1.07257100
C	1.60037600	-1.19478000	0.01772000	H	3.73574300	-1.37757200	-0.01961100
C	2.78967400	-1.91235000	0.03238300	H	1.64450100	-5.11402100	0.17804400
C	2.83760900	-3.32691800	0.10292200	H	-0.51346500	-3.89566500	0.09553700
C	1.63717000	-4.02969700	0.12148700	H	-1.18348600	3.19527700	-0.54245100
C	0.41918500	-3.34823700	0.07393300	H	-0.37712200	5.54417600	-0.47251300
C	1.63798500	0.24188800	-0.02019800	H	2.01710000	6.05270700	-0.11842200
C	0.79690700	2.38817000	-0.22072000	H	3.66522900	4.21694700	0.18517100
C	-0.13374600	3.42171800	-0.38762900	H	-0.34155000	0.54480600	-0.25290200
C	0.32979400	4.72998800	-0.34560900	C	4.16174600	-4.01719200	0.15407600
C	1.68417200	5.02035300	-0.14449900	H	4.77723700	-3.74577800	-0.71175200
C	2.61522000	3.99503700	0.02510800	H	4.72615900	-3.71497200	1.04446500
C	2.16177100	2.68373200	-0.01328800	H	4.04878300	-5.10296700	0.17108200
N	-0.79824300	-1.20785800	0.02222300				

S_2-min-M-Me-N (the S_2 minimum of M-Me in the normal form)

Energy: -1391.44305340

C	-5.17823600	-2.24770000	-0.27872900
C	-4.59639500	-2.69669500	-1.46780400
C	-3.32050700	-2.26214900	-1.82909400
C	-2.62195300	-1.38678800	-1.00846600
C	-3.20417500	-0.92749100	0.18563100
C	-4.49135300	-1.36907000	0.54281800
C	-2.51584400	-0.00525100	1.08839000
C	-0.70036900	1.52370300	0.43906600
C	0.70155200	1.65817300	0.06150800
C	1.12275200	2.92659700	-0.33720800
C	0.26298000	4.04912900	-0.35285200
C	-1.07454400	3.89458100	0.03615300
C	-1.55419500	2.64761500	0.42123300
C	1.58889700	0.52827100	0.07401300
C	2.28960500	-1.57947300	0.35172000
C	2.25531400	-2.95206200	0.67758500
C	3.40125000	-3.71033200	0.51292100
C	4.59212200	-3.14334900	0.03015600
C	4.65158300	-1.78939900	-0.29956600
C	3.50583500	-1.02126300	-0.13803100
C	0.79765700	5.37526500	-0.77965200
N	-1.14791400	0.29293800	0.75220700
N	1.26130500	-0.70862300	0.46625300
O	-2.99759600	0.48405600	2.09579600
S	3.27535400	0.67655100	-0.46407900
H	1.62776400	5.68551400	-0.13307400
H	1.20369600	5.32056500	-1.79717200
H	0.02973100	6.15050100	-0.75332900
H	-6.17061400	-2.58727500	0.00232000
H	-5.13674800	-3.38576100	-2.10988300
H	-2.86881300	-2.61021800	-2.75299500
H	-1.62851300	-1.05303300	-1.29211100
H	-4.92774800	-1.00863700	1.46874600
H	2.15278000	3.06938100	-0.65247000
H	-1.73868700	4.75273000	0.03728500
H	-2.58525600	2.52477100	0.73001000
H	1.33419700	-3.38895700	1.04998700
H	3.37972600	-4.76739100	0.76215800
H	5.47575400	-3.76224900	-0.08892100
H	5.57041800	-1.34975900	-0.67447000
H	-0.40819200	-0.45151900	0.75483400

S_0-min-M-OMe-N (the S_0 minimum of M-OMe in the normal form)

Energy: -1466.71035340

C	-4.73322000	-3.16311400	-0.44321700	N	-0.38854000	1.23081400	-0.06129500
C	-5.28833300	-2.02574200	0.14142700	O	-0.59194500	-3.71838100	-0.14070300
C	-4.45758300	-1.04849500	0.68519200	S	1.68837100	2.77796500	0.00216600
C	-3.07480000	-1.19840200	0.63399600	H	-5.37783000	-3.92927800	-0.86358800
C	-2.51256200	-2.33295900	0.03818000	H	-6.36692100	-1.90485400	0.18026800
C	-3.35305200	-3.31912400	-0.48640100	H	-4.88618100	-0.17056900	1.15942200
C	-1.03659500	-2.57750500	-0.03742700	H	-2.44236000	-0.43946800	1.08607900
C	1.11724200	-1.33529200	0.00353700	H	-2.90248100	-4.20249800	-0.92739400
C	1.70960200	-0.03961800	-0.00209700	H	3.58410200	1.04008100	0.00340000
C	3.10356400	0.06629400	0.01048000	H	3.95212200	-3.21741300	0.05182100
C	3.92937300	-1.05216900	0.03065200	H	1.50977000	-3.43286400	0.02167900
C	3.34434000	-2.32004800	0.03718200	H	-2.98562000	2.10343500	-0.15219400
C	1.96168400	-2.45083000	0.02311500	H	-3.59985600	4.51789500	-0.17112300
C	0.91398200	1.18857100	-0.02249500	H	-1.84574200	6.25910100	-0.11213700
C	-0.87272600	2.51883500	-0.07821400	H	0.55265600	5.64213500	-0.03474700
C	-2.22510100	2.87733400	-0.12412300	H	-0.74884400	-0.54165100	-0.03641000
C	-2.55581700	4.22289200	-0.13558400	O	5.26233100	-0.80876600	0.04073100
C	-1.56069700	5.21166200	-0.10258000	C	6.13246600	-1.92454400	0.06126200
C	-0.21392500	4.87486100	-0.05889200	H	7.14394200	-1.51809000	0.06703800
C	0.11860900	3.52133900	-0.04765400	H	5.98370700	-2.53417100	0.96029300
N	-0.27257200	-1.44688700	0.00444600	H	6.00159300	-2.55321600	-0.82737600

S_1-min-M-OMe-N (the S_1 minimum of M-OMe in the normal form)

Energy: -1466.59947730

C	-4.47178200	-3.48953400	-0.28120100
C	-5.08209400	-2.34504900	0.23406000
C	-4.30051500	-1.26734800	0.64717100
C	-2.91578800	-1.32130900	0.53600000
C	-2.29656200	-2.46617100	0.01060600
C	-3.08989800	-3.55332000	-0.38466300
C	-0.82900500	-2.62319900	-0.11709500
C	1.24286400	-1.25425900	-0.02061300
C	1.72840900	0.13063800	0.00567100
C	3.11068600	0.29585900	0.03859600
C	4.00126800	-0.79527200	0.05124700
C	3.52640700	-2.12371600	0.02795500
C	2.16196800	-2.32905800	-0.00788900
C	0.84521000	1.25138300	-0.00805600
C	-1.08925700	2.38562700	-0.08146900
C	-2.47652000	2.63399900	-0.14668700
C	-2.93009500	3.94329800	-0.16004600
C	-2.04040700	5.02619400	-0.11449800
C	-0.66255200	4.80719300	-0.05742200
C	-0.20102800	3.49868000	-0.04319300
N	-0.10424100	-1.43587500	-0.03608100
N	-0.49764300	1.16938800	-0.05331600
O	-0.29778100	-3.71515800	-0.29363200
S	1.44984900	2.92620500	0.01895600
H	-5.07725200	-4.33247300	-0.60041700
H	-6.16359100	-2.29582200	0.31842400
H	-4.77064500	-0.38211400	1.06495800
H	-2.32817700	-0.47590100	0.88241000
H	-2.59761900	-4.43792300	-0.77510000
H	3.55194600	1.28707800	0.05498400
H	4.20183700	-2.96904700	0.03842400
H	1.75773900	-3.33126200	-0.03245800
H	-3.16697200	1.79742700	-0.19204600
H	-3.99841300	4.13436100	-0.21002100
H	-2.42147700	6.04239100	-0.12751300
H	0.02973100	5.64285900	-0.02662600
H	-0.62210200	-0.52637500	-0.05360900
O	5.28971600	-0.46223900	0.08513500
C	6.27894400	-1.48787900	0.09646500
H	7.23657700	-0.97102000	0.12317800
H	6.17362900	-2.11799000	0.98396100
H	6.21339700	-2.09942800	-0.80772500

S$_1$-min-M-OMe-T (the S$_1$ minimum of M-OMe in the phototautomeric form)

Energy: -1466.59620178

C	-4.48510300	-3.45033900	-0.32557700	N	-0.45164000	1.23045700	-0.17002500
C	-5.06614200	-2.42597600	0.42210800	O	-0.32431200	-3.60201500	-0.64842700
C	-4.26245800	-1.42899600	0.97345400	S	1.45526900	2.91694100	0.12710300
C	-2.88691400	-1.44734500	0.76596400	H	-5.10761600	-4.23129000	-0.75294100
C	-2.29597200	-2.46665700	0.00814400	H	-6.14077700	-2.40810200	0.57937700
C	-3.10985500	-3.47450500	-0.52282100	H	-4.70784400	-0.63856600	1.57078600
C	-0.82101800	-2.54529500	-0.23161400	H	-2.25947400	-0.68498800	1.21706900
C	1.19163700	-1.25505100	-0.00744700	H	-2.63850100	-4.26831200	-1.09357100
C	1.73728500	0.09857400	0.01667100	H	3.57088200	1.23801700	0.02929600
C	3.11376700	0.25272600	0.04154000	H	4.14326100	-3.02066200	0.08276800
C	3.99545700	-0.85570900	0.07275100	H	1.69526200	-3.32986400	-0.00621400
C	3.49083600	-2.15684100	0.05639200	H	-3.15745300	1.84588900	-0.42563900
C	2.11001800	-2.33107900	0.01078500	H	-3.96191400	4.19605100	-0.40402800
C	0.89636400	1.26415300	-0.00937900	H	-2.37625900	6.07697100	-0.15077600
C	-1.09038500	2.43294600	-0.17848200	H	0.05984200	5.64874600	0.09362200
C	-2.46401000	2.67307800	-0.31427500	H	-0.83929700	0.26413100	-0.17938900
C	-2.90077800	3.99115100	-0.30018200	O	5.29191700	-0.52885400	0.11168400
C	-2.00556100	5.05725500	-0.15665200	C	6.25413400	-1.57514900	0.13296000
C	-0.63641900	4.82445100	-0.01989700	H	7.22634700	-1.08529000	0.15883100
C	-0.18972600	3.51055400	-0.03175000	H	6.13127900	-2.19942900	1.02346500
N	-0.16118200	-1.37108900	0.00821700	H	6.17593300	-2.19465400	-0.76586900

S$_2$-min-M-OMe-N (the S$_2$ minimum of M-OMe in the normal form)

Energy: -1466.58019804

C	-4.96147900	2.84551000	0.35329300	N	-1.15589900	0.03972600	-0.82937400
C	-4.30162400	3.26370800	1.51308000	N	1.30639300	0.90645300	-0.45795200
C	-3.04320200	2.74586600	1.82360100	O	-3.07895500	-0.04652300	-2.08357500
C	-2.44018000	1.81976000	0.98353300	O	0.52501300	-4.96611400	0.60502100
C	-3.10132300	1.38973300	-0.18166600	S	3.24533900	-0.62555600	0.38901700
C	-4.37095200	1.91668300	-0.48725100	H	-5.93996200	3.24906100	0.11010900
C	-2.51545600	0.41988400	-1.10532700	H	-4.76654800	3.99237800	2.17025600
C	-0.77673900	-1.21666200	-0.52074700	H	-2.52966200	3.06902900	2.72411000
C	0.60992100	-1.43649100	-0.13760600	H	-1.46013600	1.42302400	1.23009300
C	0.95759300	-2.72446700	0.23945600	H	-4.86984500	1.58049200	-1.39046600
C	0.02205400	-3.79056500	0.22630200	H	1.96429200	-2.96054800	0.56853900
C	-1.30844600	-3.57816300	-0.15958700	H	-2.02950300	-4.38488200	-0.18461100
C	-1.69239900	-2.29231200	-0.52099800	H	-2.71083400	-2.10339900	-0.83718300
C	1.56674500	-0.35721300	-0.12020500	H	1.53052300	3.59841400	-0.94154900
C	2.38834900	1.71318600	-0.32595300	H	3.65520800	4.84645900	-0.62954100
C	2.42915400	3.09534000	-0.59870500	H	5.69911300	3.69038400	0.15449600
C	3.61921400	3.78103500	-0.42087800	H	5.65959600	1.25540300	0.64571000
C	4.77960300	3.12880300	0.02337400	H	-0.38762100	0.74584200	-0.79953600
C	4.76378900	1.76172400	0.30018000	H	0.29365400	-6.93164300	0.97411200
C	3.57312500	1.06839300	0.12468700	H	-1.15572900	-5.95163300	1.33227500
C	-0.32801600	-6.10530200	0.63369100	H	-0.71828700	-6.32235000	-0.36499100